1 FAA-72-2

Corrected Copy
p. A-3 Fig. 12
Reference copy

REPORT NO. DOT-TSC-FAA-72-2

VORTEX SENSING TESTS AT NAFEC

D. BURNHAM, J. HALLOCK,
R. KODIS, T. SULLIVAN
TRANSPORTATION SYSTEMS CENTER
55 BROADWAY
CAMBRIDGE, MA 02142

TECHNICAL REPORT
JANUARY 1972

transpo 72
U.S. International Transportation Exposition
Dulles International Airport
Washington, D.C.
May 27-June 4, 1972

Prepared for:

DEPARTMENT OF TRANSPORTATION
FEDERAL AVIATION ADMINISTRATION
WASHINGTON, D.C. 20590

1. Report No. DOT-TSC-FAA-72-2	2. Government Accession No.	3. Recipient's Catalog No.
4. Title and Subtitle VORTEX SENSING TESTS AT NAFEC		5. Report Date January 1972 6. Performing Organization Code
7. Author(s) D. Burnham, J. Hallock, R. Kodis, T. Sullivan		8. Performing Organization Report No.
9. Performing Organization Name and Address Department of Transportation Transportation Systems Center 55 Broadway, Cambridge, MA 02142		10. Work Unit No. R-2102 11. Contract or Grant No. FA-205
12. Sponsoring Agency Name and Address Department of Transportation Federal Aviation Administration Washington, D.C. 20590		13. Type of Report and Period Covered Technical Report June 15-July 15,1971 14. Sponsoring Agency Code
15. Supplementary Notes		

16. Abstract This report describes the results of a series of tests conducted for the FAA at NAFEC by the DOT/Transportation Systems Center. The test objectives were to determine and evaluate some of the characteristics of three experimental techniques for the remote sensing of the wing-tip vortices generated by heavy commercial and military aircraft. These techniques involved (1) a pulsed, bistatic acoustic detection and ranging system (referred to as an acoustic radar); (2) a ground level pressure sensor; and (3) a ground level hot-wire anemometer. The tests were conducted both in conjunction with the instrumented tower and at the end of runway 13. Data were obtained and analyzed for a variety of aircraft including the DC-7, B-747, C-141 and C-5A. Results in the form of altitudes and times of tower hits and vortex tracks are presented and compared to the tower data wherever possible.

17. Key Words
Vortex
Acoustic
Sensor
Pressure

18. Distribution Statement
Availability is Unlimited. Document may be Released To the National Technical Information Service, Springfield, Virginia 22151, for Sale to the Public.

19. Security Classif. (of this report)	20. Security Classif. (of this page)	21. No. of Pages	22. Price
Unclassified	Unclassified	72	

TABLE OF CONTENTS

LIST OF ILLUSTRATIONS

LIST OF TABLES

SUMMARY

During the summer of 1971 a series of vortex sensor tests was conducted at NAFEC by personnel of the DOT/Transportation Systems Center. Three types of remote sensors were tested:

1. A bistatic pulsed acoustic radar.*
2. A ground level pressure sensor.
3. A ground level hot-wire anemometer.

The test results will be described in detail in the body of this report. The conclusions that have been drawn from these results are given below.

ACOUSTIC RADAR SENSOR

For 15 DC-7 runs made on July 8, 1971, for which both radar and tower data were obtained, the locations of the wake vortices (time and altitude of tower hit) as measured with the bistatic pulsed acoustic radar developed at TSC are generally in good agreement with the NAFEC tower data. The remaining 9 runs on that day either missed the tower or did not yield good radar and/or tower data.

From July 7 through July 15 during a series of 169 runs at NAFEC's runway 13, it was found that the vortices generated by landing aircraft can be tracked over lateral distances of up to 1000 feet using a relatively small number of acoustic transducers. The principal limiting factor was the measurement of the time of arrival of the ground pulse, which was strongly affected by ground attenuation and low-level wind shear.

PRESSURE SENSORS

Measurements with the ground level pressure sensor showed that the pressure change produced at the ground by a vortex can be used to detect its passage at altitudes below about 100 feet.

---

*Strictly speaking the word "radar" is a misnomer. Analogous terminology would lead to neologisms like "acdar" or "sodar", neither of which is part of the current technical vocabulary. "Sonar" is inaccurate since it stands for (underwater) Sonic Navigation and Ranging. We have therefore adopted "acoustic radar" as being no more inaccurate and perhaps more descriptive.

The magnitude of the pressure change as a function of the altitude measured by the acoustic radar agrees well with calculations from elementary vortex theory.

These results have led to a plan to test an array of ground level pressure sensors as a means of tracking the lateral displacement of low altitude vortices.

VELOCITY SENSORS

The hot-wire anemometer data indicate that ground level wind measurements are less reliable than pressure measurements in detecting the passage of a vortex.

INTRODUCTION

During the periods from June 14-18 and from July 6-16, 1971, tests were conducted at NAFEC to determine the utility and accuracy of several aircraft vortex sensing systems developed at TSC. Two groups of tests were carried out as outlined in Table 1. In the first, vortices generated by a NAFEC DC-7 (Fig. 1) were measured simultaneously by the TSC sensors and by the NAFEC instrumented tower (Fig. 2). In the second group, the vortices generated by a variety of aircraft, including some specially arranged Pan Am training flights, were measured at the approach end of runway 13 (Figs. 3 and 4).

TABLE 1. NAFEC TEST SUMMARY

Date	DC-7				
6/15*	9				
6/17*	12				
7/8	24				
Total	45				
TOTAL AT TOWER: 45 RUNS					
Date	747	707/DC-8	C-5A	C-141	Other
7/7		18			13
7/12*			1		
7/13	24	3	9	4	9
7/14	3	9		14	
7/15	11	12		34	5
Totals	38	42	10	52	27
GRAND TOTAL AT RUNWAY 13: 169 RUNS					
*Pressure and velocity sensors not set up for measurements.					

Three different sensors were tested: (1) a bistatic pulsed acoustic radar; (2) a ground level pressure sensor; and (3) a ground level hot-wire anemometer. The acoustic radar had been previously developed in experiments at TSC and at the Logan International Airport; the pressure sensor and the anemometer had not been tested previously for vortex detection. All sensors were operated by TSC personnel from the self-contained mobile laboratory van shown in Figure 1.

Figure 1. DC-7 and Mobile Laboratory Van (Run 16, 7/8/71

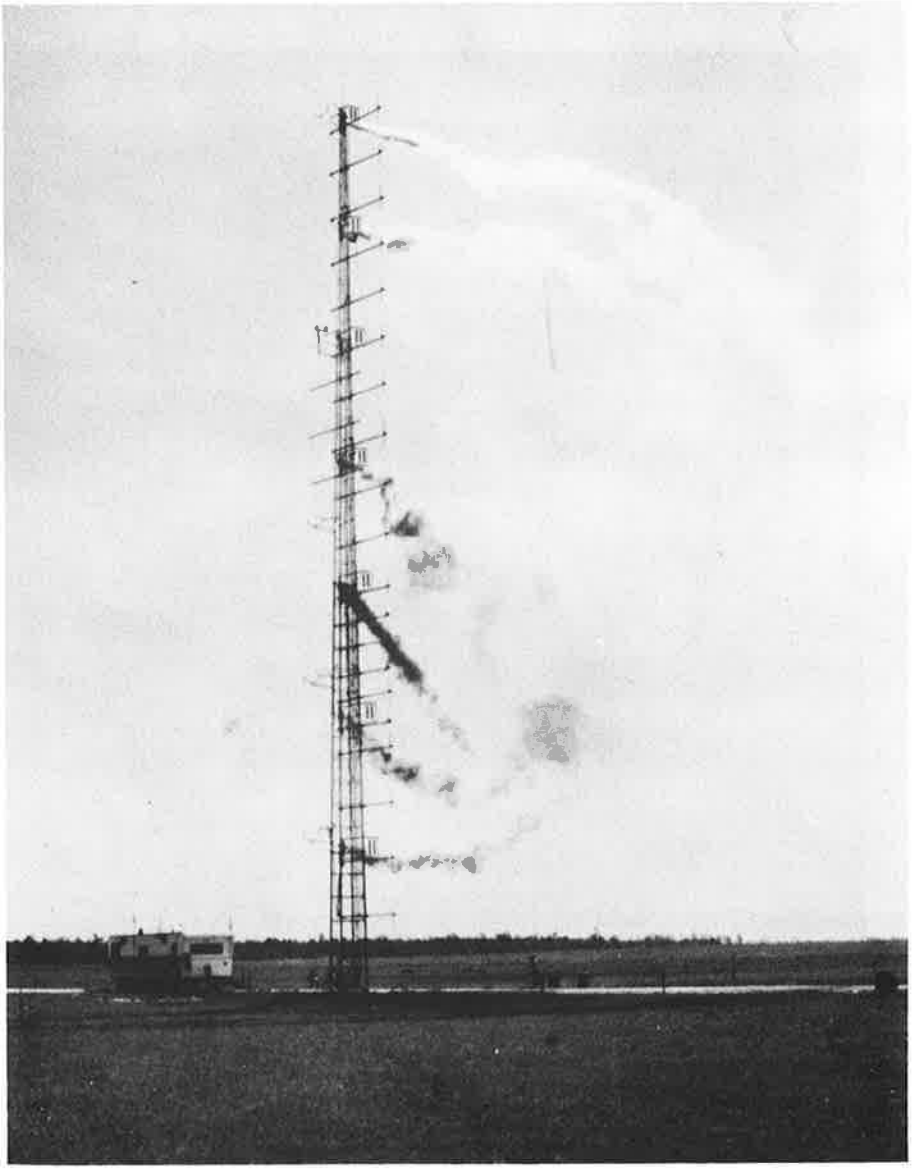

Figure 2. NAFEC Tower with Smoke Visualization (Run 14, 7/8/71)

Figure 3. Pan Am 747 Approaching NAFEC Runway 13

APPROACH END OF NAFEC RUNWAY 13

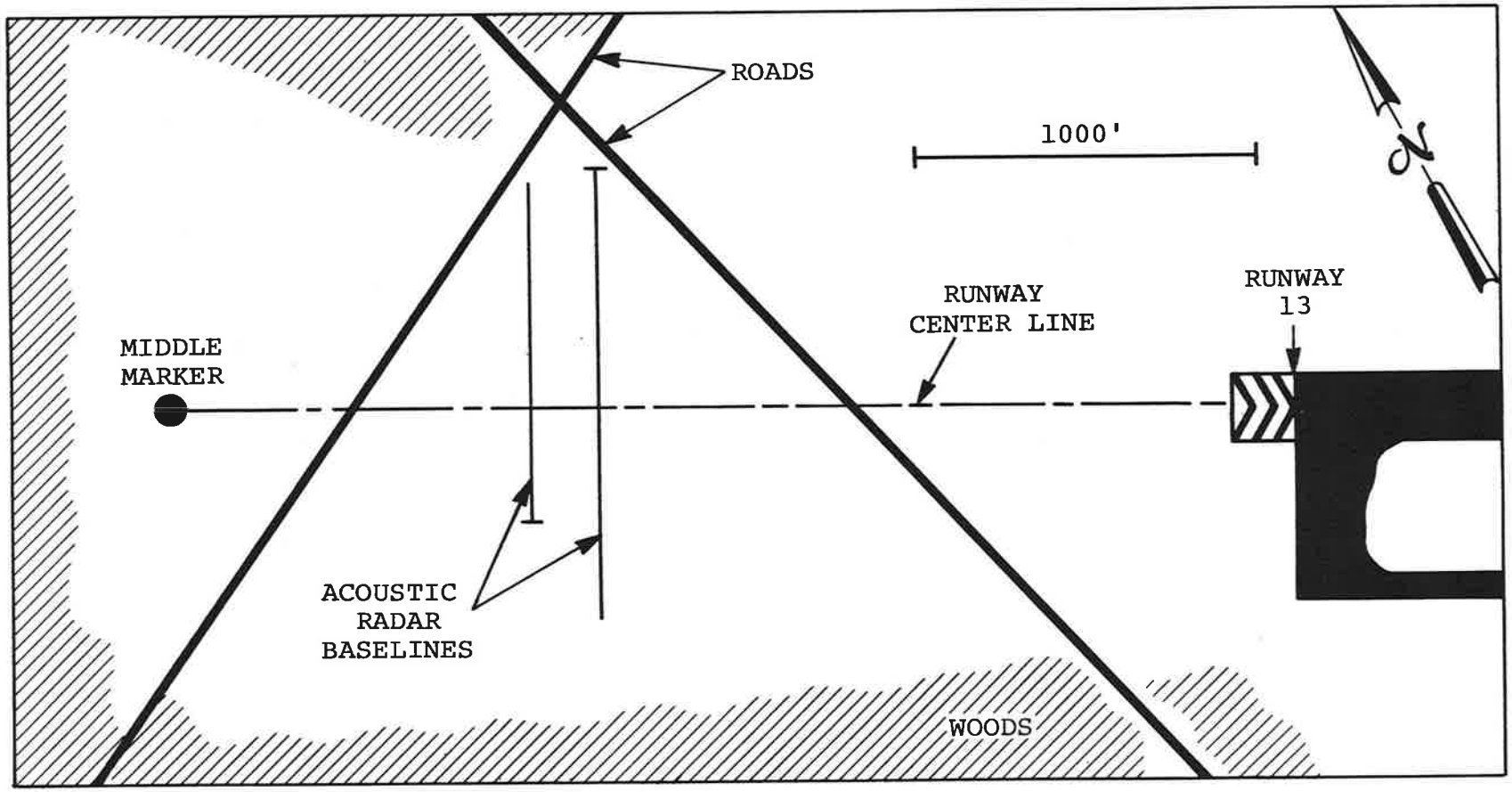

Figure 4. Test Site at NAFEC Runway 13

Four goals were set for these tests:

- To determine the accuracy of the vortex locations measured by the acoustic radar system.

- To establish the ability of the acoustic radar to track vortices over distances longer than those available at Logan.

- To establish the utility of ground based pressure and velocity sensors.

- To measure the maximum distance that vortices may travel before dissipation under various weather conditions, especially vortices generated by the largest jet transports (B-747 and C-5A).

Some progress was made toward each of these goals, though none was completely achieved. An additional important result of these tests, not included in the above, was that they made evident a number of ways in which the basic acoustic radar could be improved. These improvements are being effected, and further tests are being planned at Kennedy Airport and at NAFEC in the near future.

NAFEC TESTS WITH THE BISTATIC PULSED ACOUSTIC RADAR

The physical basis of the acoustic radar developed and tested at TSC is that acoustic waves interact strongly with the intense wind field inside a vortex. This interaction leads to the bending of the sound rays (or rotation of the wave front) in the direction of rotation of the vortex core, and the refraction or scattering of the sound away from the original direction of propagation. For a given direction of propagation, only one of the two counter-rotating vortices scatters the incident sound back down to the ground, as shown in Figure 5. For the other vortex to do the same the incident wave must come from the opposite direction, i.e., transmitter and receiver must be interchanged.

It can be shown that there is a maximum angle through which refractive scattering of this kind is possible. Typical experimental values for various aircraft in a landing configuration are given below:

Aircraft Type	Max. Scattering Angle
DC-9, B-727, BAC-111	1.2 rad.
B-747	1.0 rad.
DC-8, B-707	0.5 rad.

It can be shown that these angles are directly proportional to the vortex strength and inversely to the radius of the core. Thus, the vortex of a DC-9 with a small core scatters much more strongly than a DC-8 vortex with a much larger core, even though the DC-9 vortex strength is only half that of a DC-8.

DESCRIPTION OF THE RADAR

The basic bistatic radar consists of a sound transmitter at one side of a runway emitting sound pulses into a vertical fan beam. The pulse carrier is in the mid-audio band (~ 3KHz); the pulse duration is 2 milliseconds and the prf is about 10 per second. The acoustic receiver is on the opposite side of the runway from the transmitter. Its antenna pattern is also a fan beam, co-planar with the transmitter beam. When a vortex with appropriate characteristics intersects the sensitive region in the plane of the radar, the receiver detects two pulses for each one that is transmitted. The initial response is to that portion of the pulse which travels parallel to the ground; the second is to that portion which is refracted downwards by the vortex and, since it has travelled farther, arrives later. The

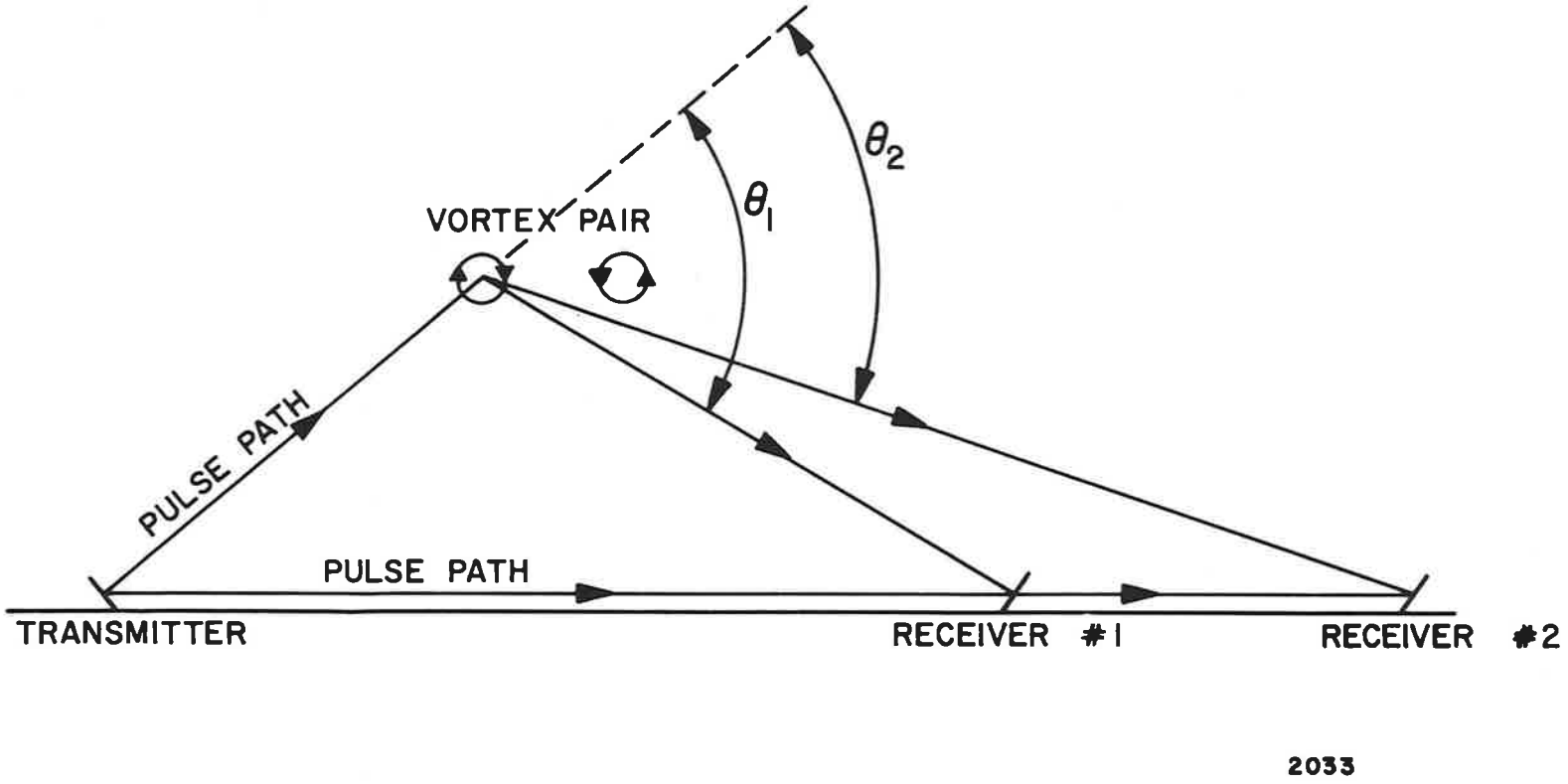

Figure 5. Pulsed Acoustic Bistatic Radar

measured value of the time-delay difference, τ (tau), determines an elliptical locus, with foci at the transmitter and receiver, for which τ is a constant and on which the vortex is located. A second receiver, displaced from the first, provides a second delay difference and determines a second elliptical locus for the vortex. The intersection of the two is both necessary and sufficient to determine a unique vortex location.

The transmitters and receivers used in these measurements are shown in Fig. 6. Most often these consisted of a loudspeaker or a microphone mounted at the focus of a cylindrical parabolic reflector (Figs. 6a and 6b). These reflectors form a beam with a horizontal width of 5° and a vertical width of 45° at 3KHz. At other times an array of microphones was arranged near the focus of a parabolic dish (Fig. 6c). These microphones formed a vertical fan of pencil beams 5° wide and were used for directional measurements. The complete two way system at runway 13 included a pair of directional microphones without reflectors (Fig. 6d).

DESCRIPTION OF THE TESTS

Outline of the Test Program

The test program for the acoustic radar at NAFEC was designed to serve a two-fold function:

1. To confirm and extend preliminary results obtained with the acoustic radar at Logan International Airport.

2. To measure the ability of the radar to track accurately one or both vortices of a pair and to obtain data on their dissipation times.

Tests in conjunction with the instrumented tower were carried out on June 15 and 17 and on July 8. Unfortunately no data were obtained from the tower for the June runs. On July 8, however, both the radar and the tower were operational, and 24 DC-7 runs were observed. Details of these runs and of the radar set-up are given in Appendix C.

On July 7 and during the period July 12-15 the acoustic radar was set up near Runway 13 and data were recorded on a total of 169 runs made by a variety of heavy jets. Of these runs, 48 were made by a B-747 and a C-5A. During many B-747 and B-707 runs communications were established with the cockpit and data were received on weight, speed, configuration, radar altitude, etc. The range was set up to make it possible to track both vortices in the vicinity of the runway as well as

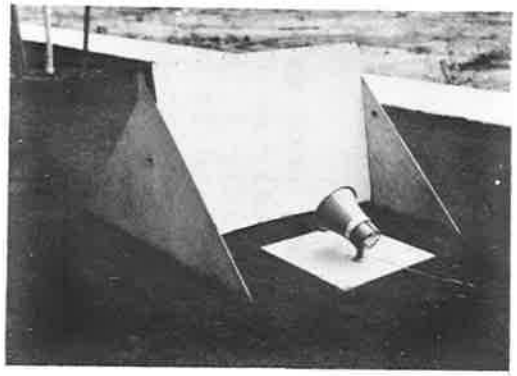

(a)

(b)

(c)

(d)

Figure 6. Acoustic Transmitters and Receivers

to detect their presence in at least one receiver at lateral distances up to 500 feet from the centerline. The long baselines gave rise to unforseen problems of pulse detection, but a considerable amount of good data were obtained nevertheless. Representative results are analyzed and presented in this report.

Outline of the Test Procedures

Data for the 24 runs of July 8 were collected as follows:

1. NAFEC tower anemometers spaced at 4 foot intervals along the 140 foot tower measured the tangential wind speed as a function of time.

2. NAFEC photo-theodolites measured the position of the nose of the aircraft as it passed the tower.

3. TSC personnel recorded acoustic radar data on the starboard vortex from the time the aircraft crossed the plane of the radar until no further delayed pulses could be observed.

From the NAFEC data it is possible to determine the altitude and displacement of the flight axis of the aircraft and the time and altitude for maximum recorded tangential velocity. The radar data yield an observed track for the starboard vortex (Figs. 7-11). Both sets of data can be reduced to values of elapsed time and altitude at which the core of the starboard vortex hit the tower. The two sets of data were recorded, analysed and reduced independently at NAFEC and at TSC. The results are tabulated in Table 2.

For the series of tests conducted at the approach to runway 13 a two-way system was set up as shown in Figure 4. A transmitter was located at one end of each baseline, as indicated. Two microphones were used on the left baseline and three on the right. Signals from these five microphones, the transmitted signal pulse, and information about aircraft type and arrival time were recorded on a seven-channel tape recorder. These data were subsequently processed to determine the vortex locations as a function of elapsed time after aircraft passage. Two vortex tracks produced in this way are shown in Figures 12 and 13 for different wind conditions. The data reduction procedure is described in Appendix A. The vortex signals observed are summarized in Appendix B.

TABLE 2. TEST RESULTS WITH DC-7, JULY 8, 1971
(TSC and NAFEC Data Independently Reduced)

RUN NUMBER		ARRIVAL TIME (SEC)		HEIGHT (FT)		INITIAL HEIGHT (FT)			*CONFIG-
TSC	NAFEC	TSC	NAFEC	TSC	NAFEC	THEOD	VORTEX	DIFF	URATION
1	29	35±5A†	R‡	55±10	R	169	168±3	1±3	H
2	30	50±8A	16(55V§)	50±5	48(60V)	162	160±3	2±3	H
3	31	≈47P#	51	32±8	48	177	P	-	T
4	32	R	25	R	108	185	R	-	L
5	33	R	57	R	108	171	R	-	H
6	34	P	M+(40V)	P	M(80V)	182	P	-	T
7	35	M	M	30	M	189	160±8	29±8	L
8	36	≈43P	M	50±8	M	123	122±2	1±2	H
9	37	25±5	R(35V)	25±8	R(40V)	99	84±4	15±4	T
10	38	11±4	21(15V)	75±8	44(80V)	102	86±6	16±6	L
11	39	31±4	30	66±5	76	79	79±2	0±2	H
12	40	R	26	R	48	78	R	-	T

† A - May not have reached tower
‡ R - Recorder was not operating
§ V - Visual observation
# P - Poor acoustic data
+ M - Missed tower

*H - Holding
L - Landing
T - Takeoff

TABLE 2. TEST RESULTS WITH DC-7, JULY 8, 1971 (Cont.)
(TSC and NAFEC Data Independently Reduced)

RUN NUMBER		ARRIVAL TIME (SEC)		HEIGHT (FT)		INITIAL HEIGHT (FT)			CONFIG-URATION
TSC	NAFEC	TSC	NAFEC	TSC	NAFEC	THEOD	VORTEX	DIFF	
13	41	12±2	17	37±8	44	68	P	-	L
14	42	5.5±2	16	40±5	44	39	40±5	-1±5	H
15	43	11±3	16	30±5	32	59	40±5	19±5	T
16	44	20±5	16	75±8	60	60	P	-	L
17	45	A	22	30	44	76	P	-	H
18	46	16±2	22	47±8	60	68	49±5	19±5	L
19	47	P	17	P	44	116	99±5	17±5	T
20	48	10±2	10	60±5	72	106	P	-	L
21	49	16±3	15	60±8	76	139	119±2	20±2	L
22	50	15±5	16	45-90	76	159	140±5	19±5	L
23	51	8±2	7.5	118±8	140	172	150±3	22±3	L
24	52	13±2	15	90±10	72	179	156±3	23±3	L

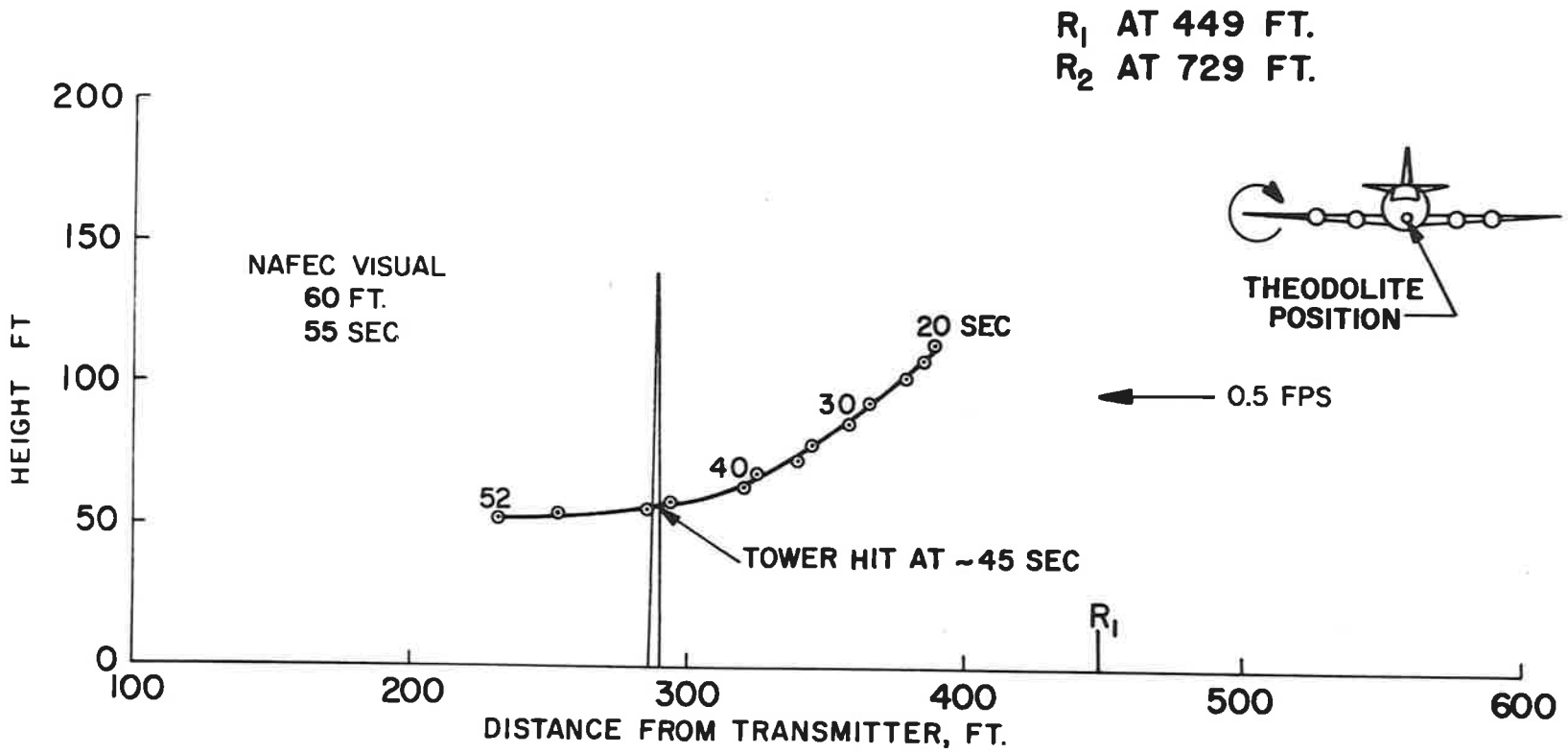

Figure 7. Run 2, 7/8/71, Tower

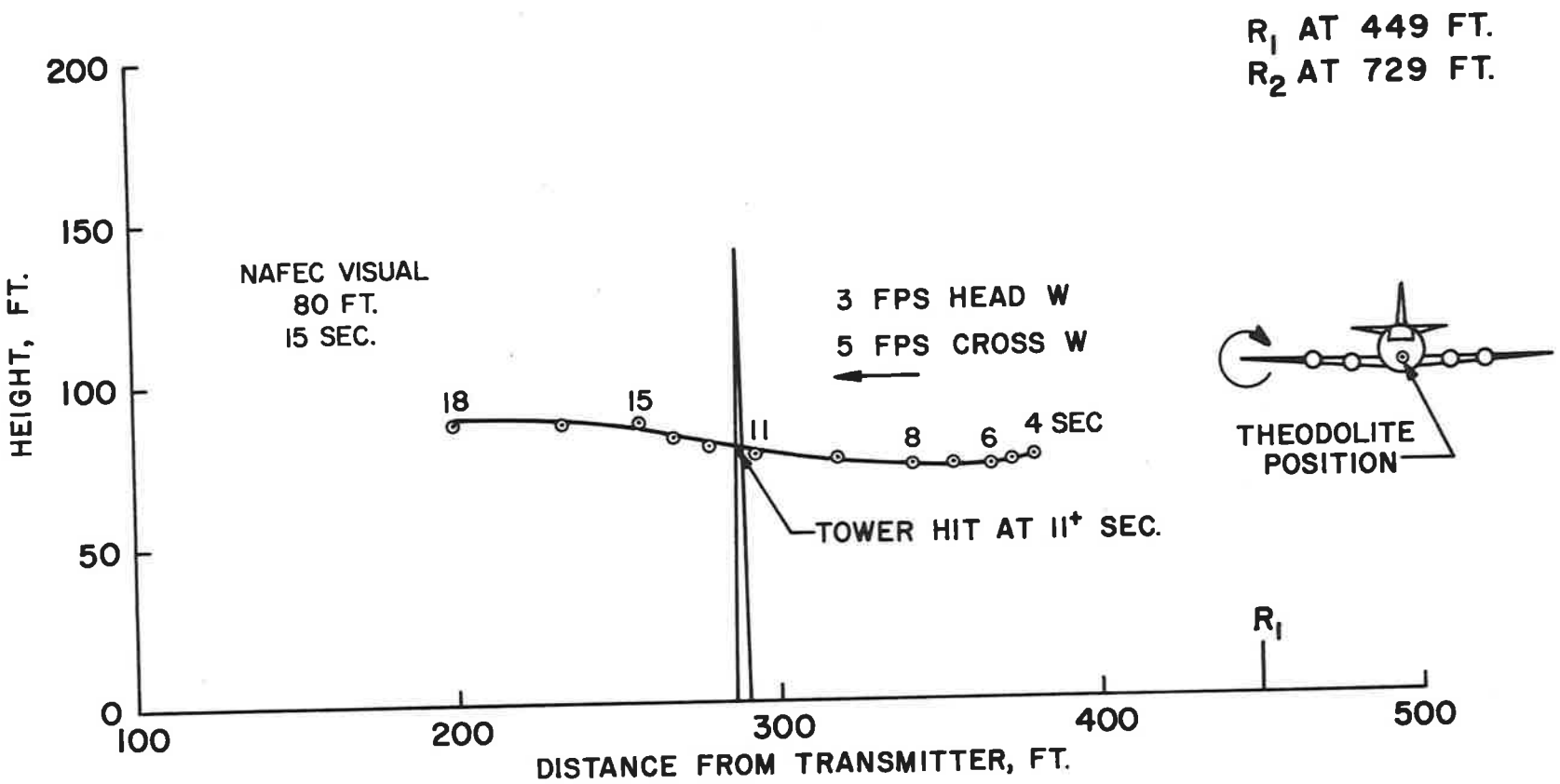

Figure 8. Run 10, 7/8/71, Tower

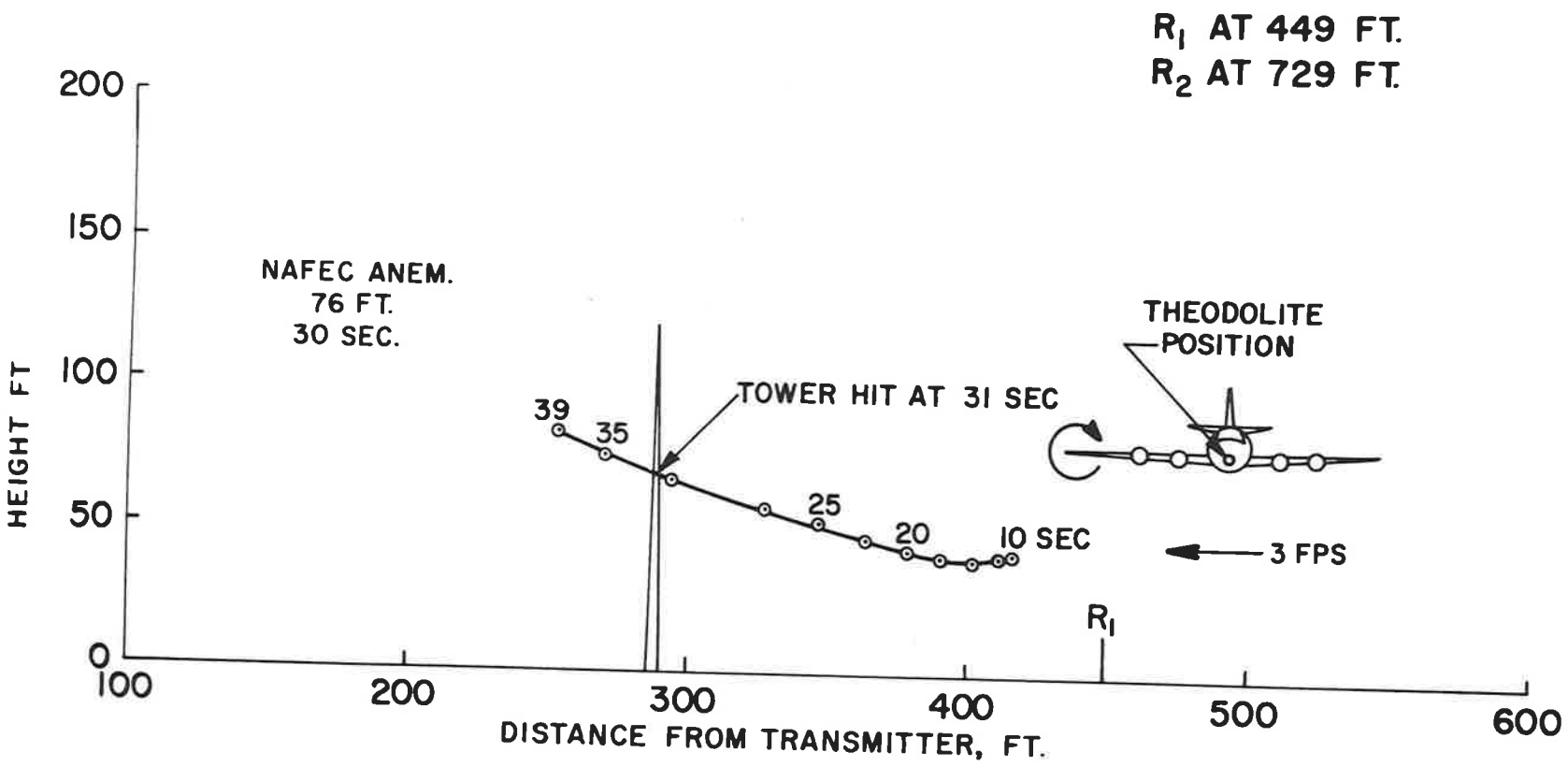

Figure 9. Run 11, 7/8/71, Tower

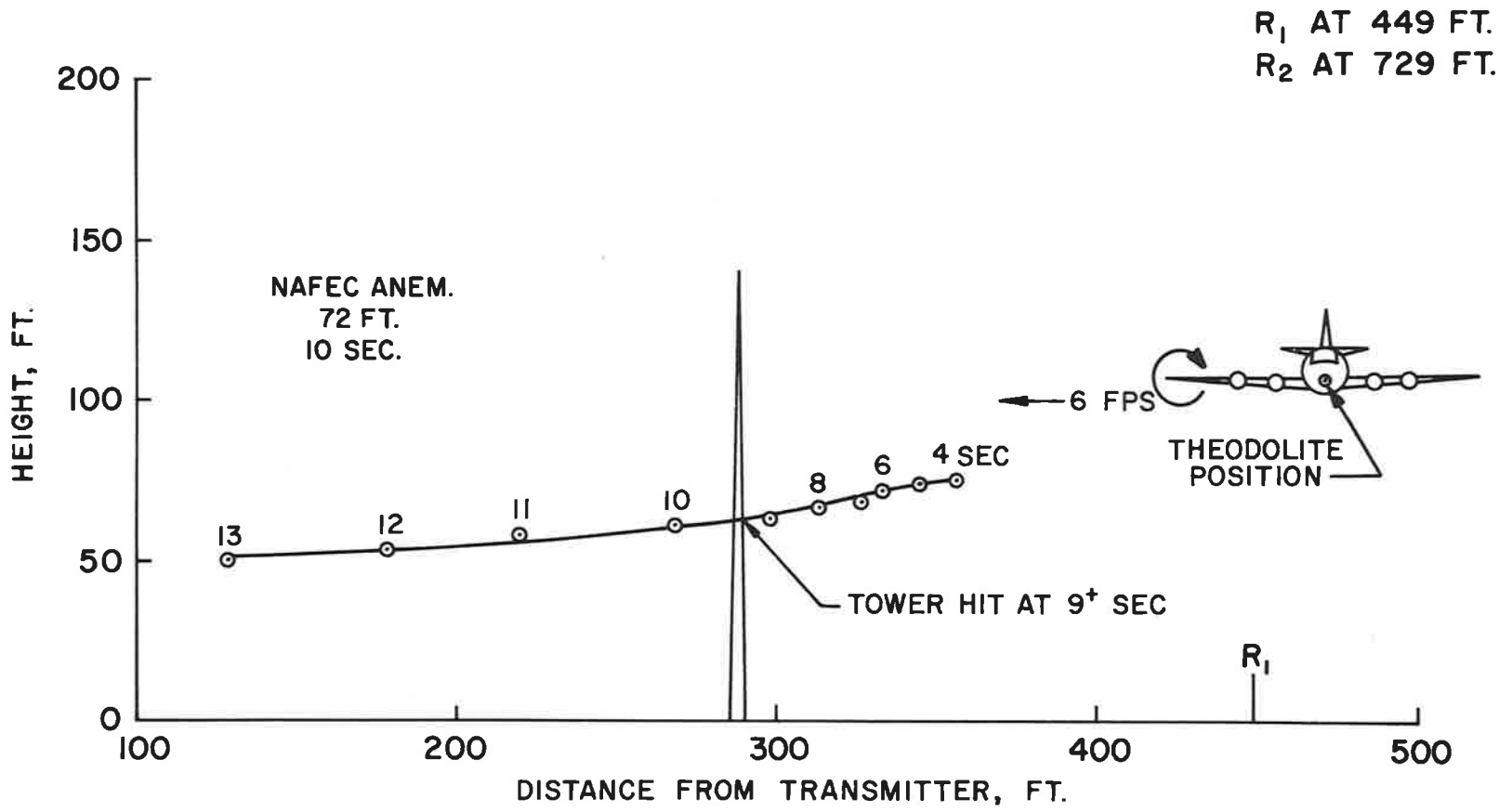

Figure 10. Run 20, 7/8/71, Tower

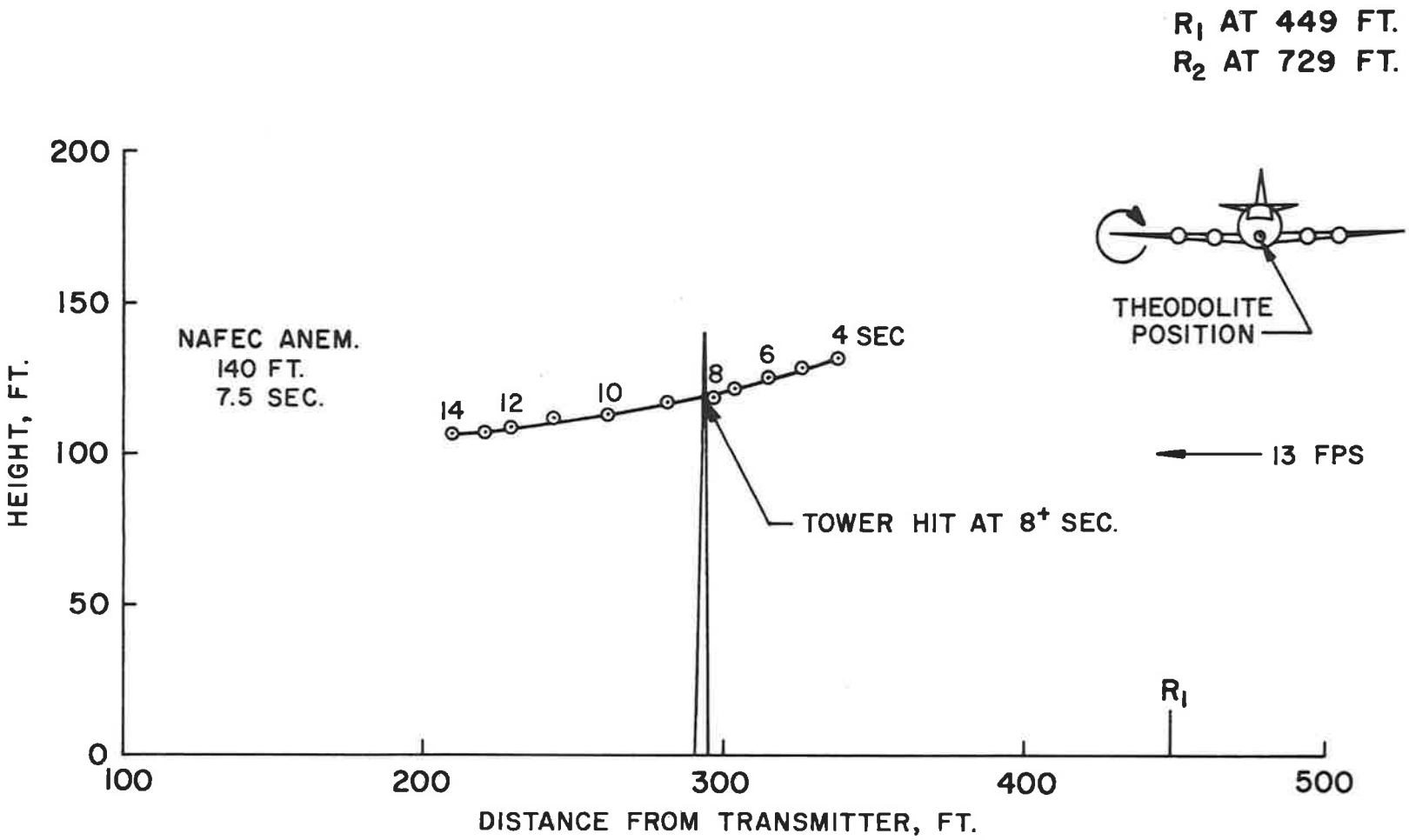

Figure 11. Run 23, 7/8/71, Tower

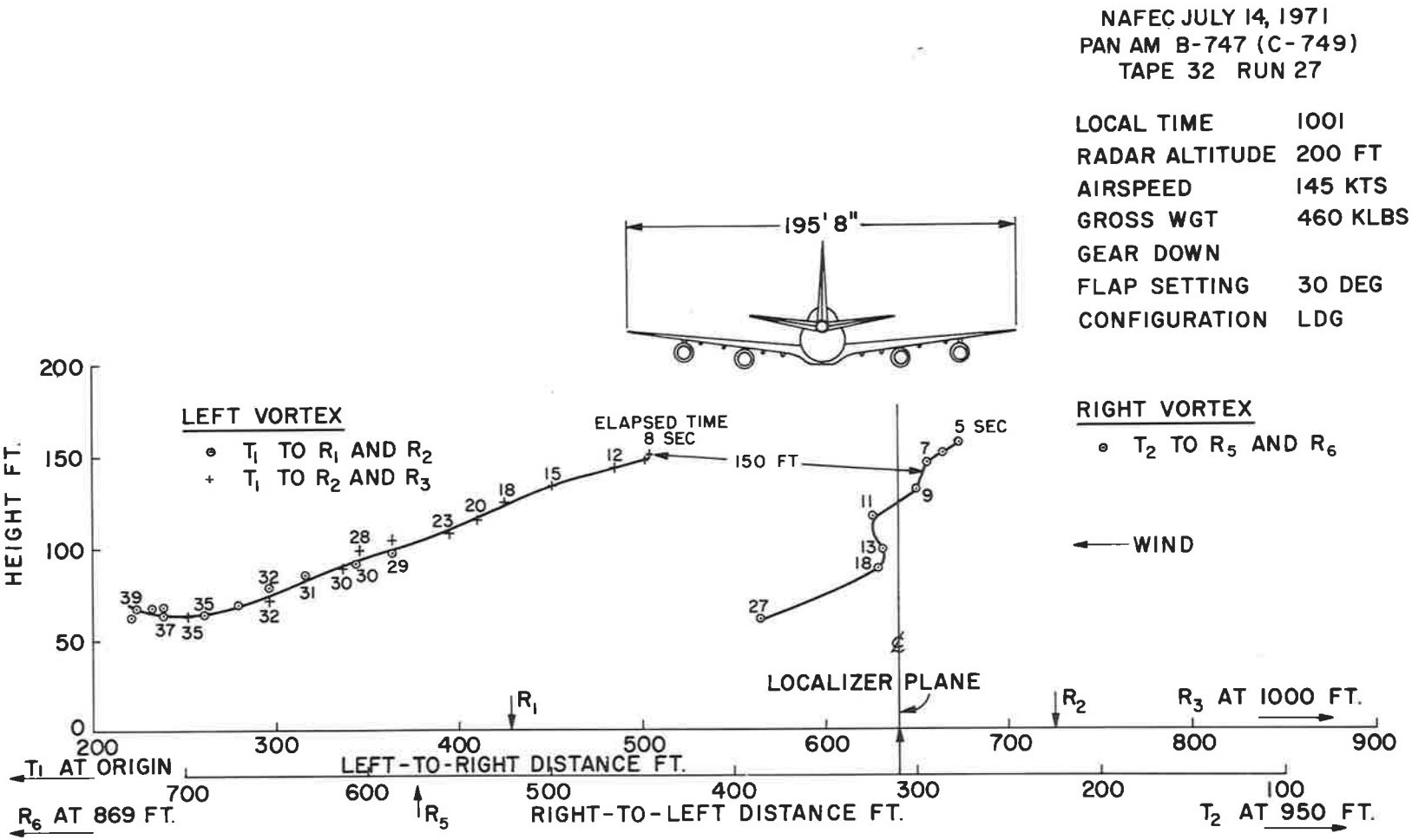

VORTEX TRACKS B - 747
NOMINAL VORTEX SPACING 155 FT.

Figure 12. Run 27, 7/14/71, Runway 13

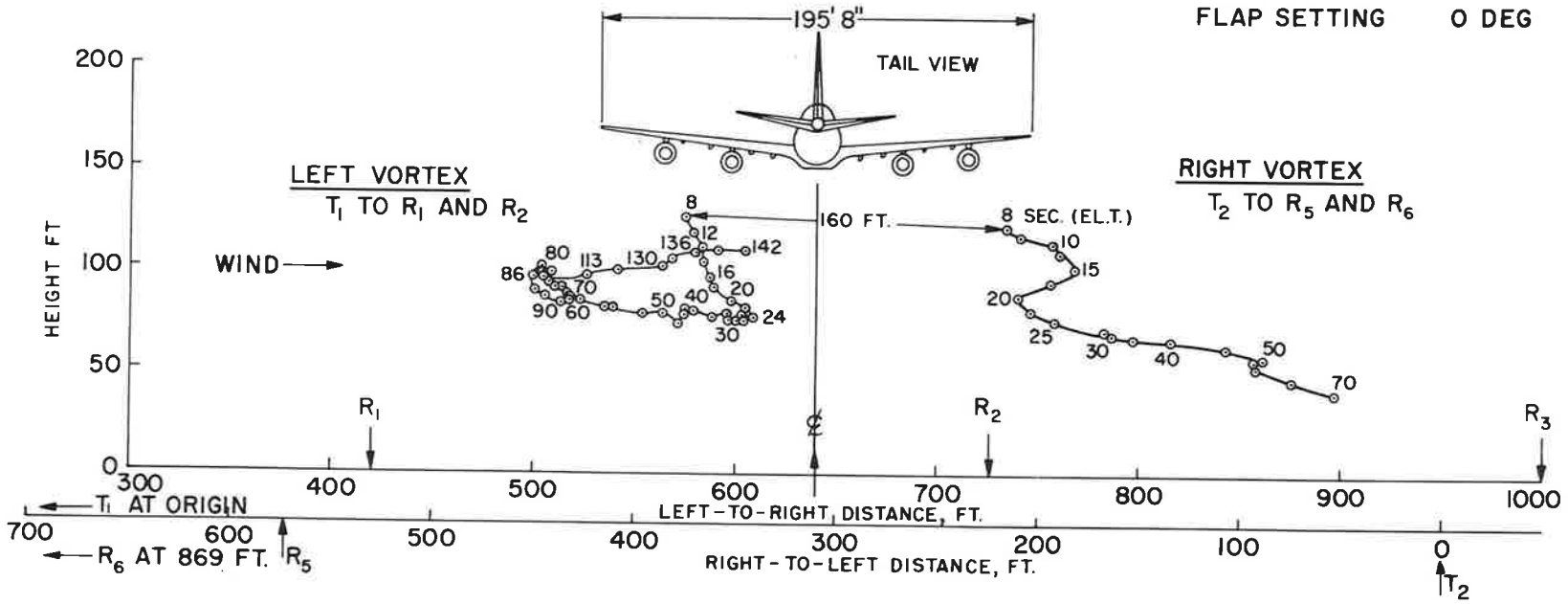

VORTEX TRACKS B-747
NOMINAL VORTEX SPACING 155 FT.

Figure 13. Run 12, 7/15/71, Runway 13

DISCUSSION OF RESULTS

Comparison of Radar and Tower Measurements

Acoustic radar measurements of the time and height of tower hits are plotted against the tower data in Figures 14 and 15. The agreement is generally quite good. In two cases (runs #2 and #10) visual estimates by NAFEC personnel agree better than the anemometer data with the radar measurements, probably because the port and starboard vortices were not correctly identified at the tower. It is evident from the plots that the radar determinations of height and arrival time tend to be lower and earlier than the values measured at the tower, 7.5 feet lower and 3 seconds earlier on the average. As plotted, the root-mean-squares of the differences are 13 feet and 5 seconds, respectively. If the tower values are reduced by the amount of the average discrepancy (or the radar values increased), the rms differences are only 9 feet and 4 seconds. In future tests of this kind at NAFEC an attempt should be made to locate the source of this apparently systematic discrepancy.

It should be noted that the above treatment of the measurement errors does not take into account the dependence of the precision of the acoustic radar on the vortex location relative to the transmitter and receivers. The errors in the radar values given in Table 2 are an estimate of this precision based upon the known uncertainty in the acoustic data for each run.

A second comparison that can be made between the NAFEC data and the radar measurements is between the altitude of the nose of the aircraft as determined from photo-theodolite positions and the initial height of the vortex as determined by a straight line extrapolation from the radar data. The procedure makes use of the fact that the low level of noise generated by the DC-7 enables the acoustic sensor to detect vortex signals in the remote receiver R_2 (Figure A-1) within a very few seconds after the aircraft passed through the radar beam. Since the vortex is initially located near the center of the T-R_2 baseline, the observed time delay is insensitive to small horizontal displacements and yields accurate height measurements during the initial uniform drop of the vortex. By extrapolating the measured values back to zero time, it is possible to determine an approximate altitude for the starboard wing-tip of the aircraft. These vortex altitudes are listed in Table 2, together with the corresponding theodolite positions of the nose. It is remarkable that the discrepancies are consistently about one foot for the holding configuration and about 20 feet for the landing or take-off configurations. The 20 foot difference is presumably accounted for by the increased angle of attack and the pitched-up nose for the two latter configurations.

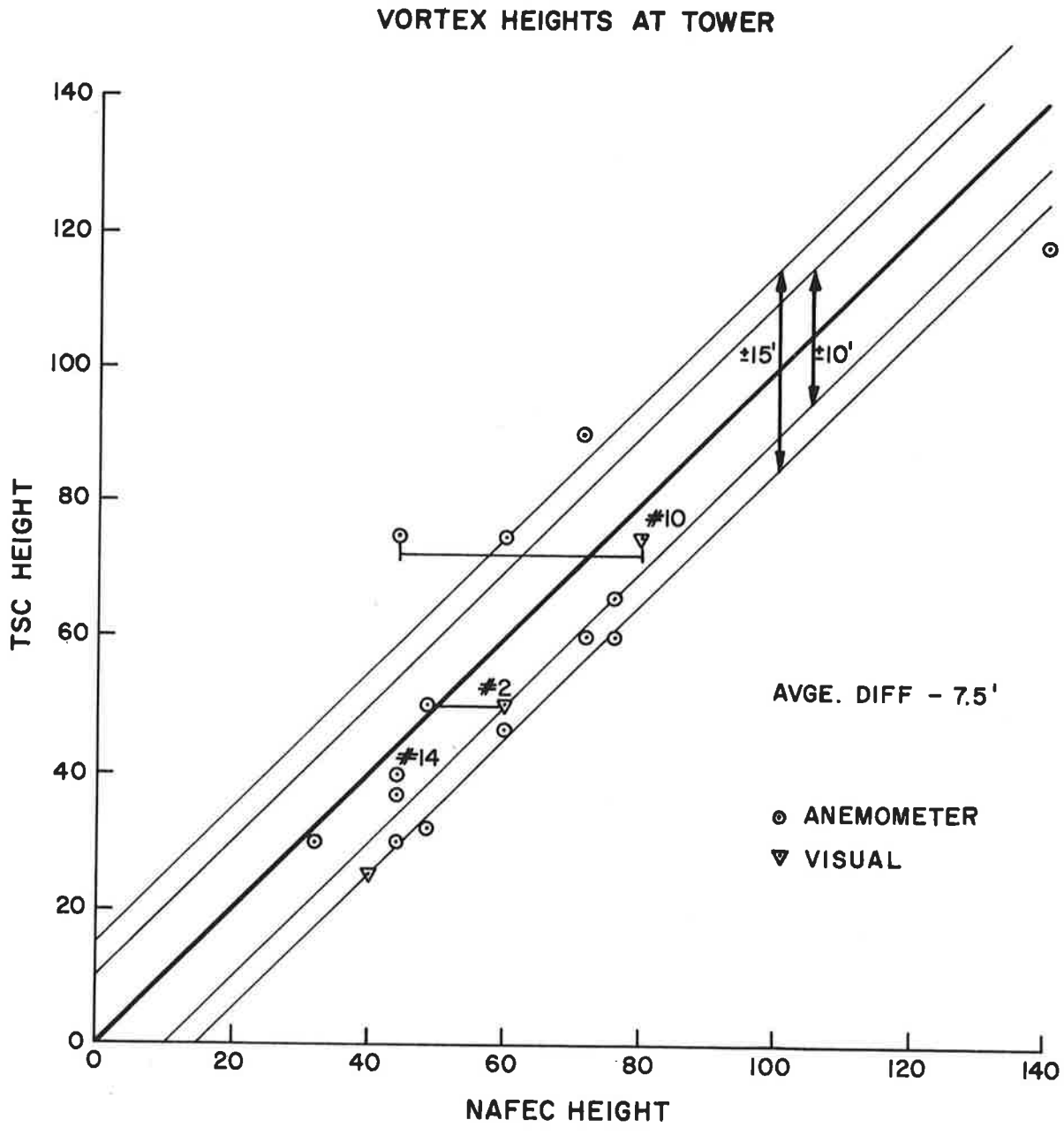

Figure 14. Comparison of Results: Vortex Heights at Tower

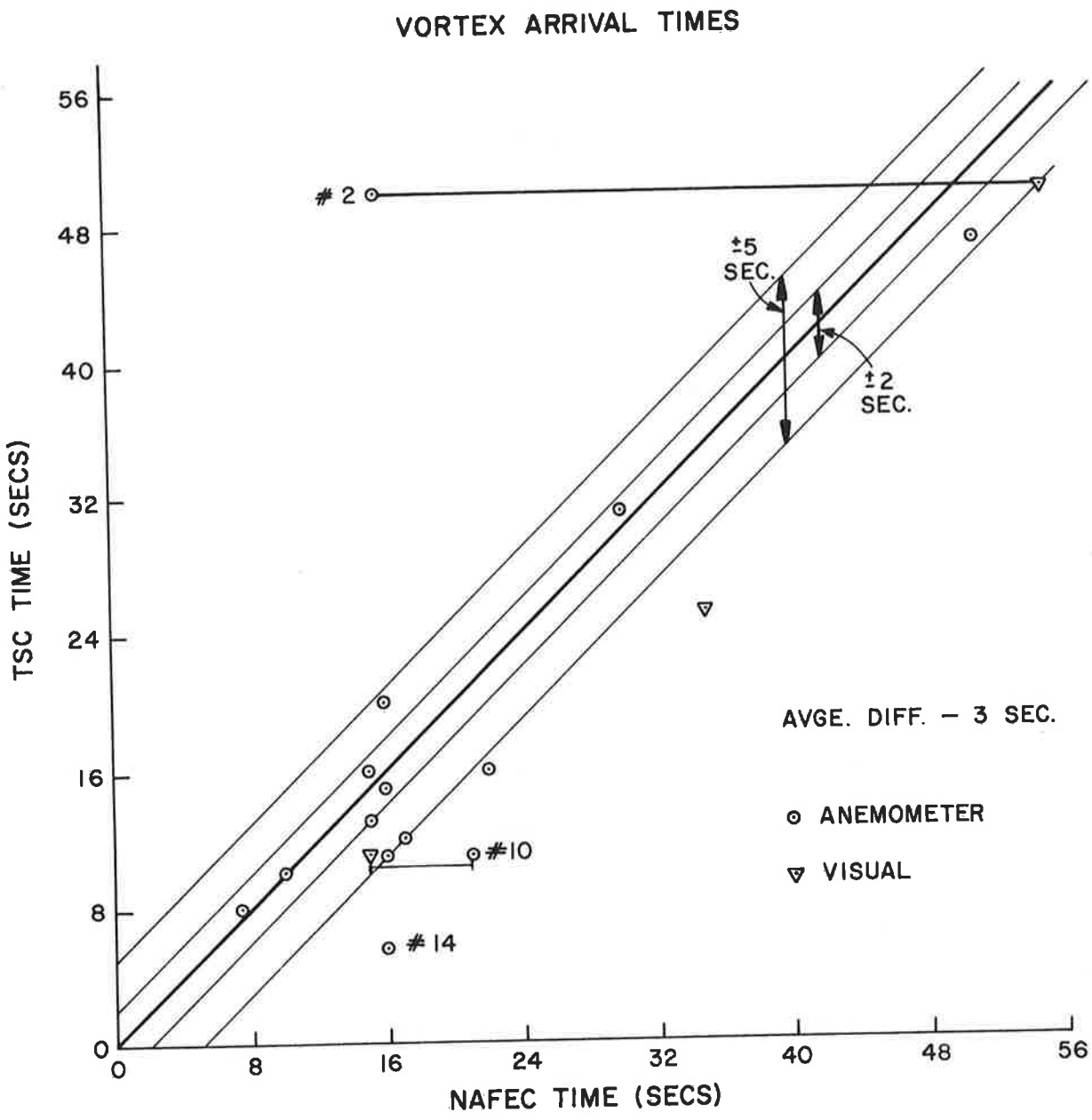

Figure 15. Comparison of Results: Vortex Arrival Times at Tower.

Vortex Tracking Results at Runway 13

An example of the acoustic data that were obtained at NAFEC runway 13 is shown in Figure A-1 in the form of an acoustogram produced from a tape recording of the receiver outputs. The procedure for reducing this pictorial data to vortex tracks in the plane of the radar is outlined in Appendix A.

Two typical pairs of tracks for two B-747 runs are shown in Figure 12 and 13. The first of these shows how both vortices are transported in the same direction by a moderate and fairly uniform wind. The left vortex has cleared the runway in less than 15 sec; the right vortex remains near the runway, and after 27 secs has dropped to an altitude of about 50 feet. It should also be noted that the upwind vortex drops more rapidly than the one downwind. This is a commonly observed feature which lacks an adequate theoretical justification.

The tracks shown in Figure 13 derive from data obtained in the early morning under light and variable wind conditions. Loss of track for both vortices occurs when they have drifted out of the sensitive volume of the radar. The right vortex could not be tracked after 70 secs, when it had dropped to an altitude of less than 50 feet and drifted over transmitter T_2, whose pulses are deflected downward by this vortex. The left vortex, after 142 secs, drifted too close to receiver R_2 and out of the sensitive volume of T_1-R_2 so that it could no longer be tracked. However, scattered signals continued to be observed over T_1-R_3 for 180 secs when they were wiped out by the noise of the following aircraft. This track shows that the organized vortex flow may persist for an extended time under the right wind conditions.

The vortex tracks plotted in Figure 13 persisted for a longer time than any others measured during the tests at runway 13. They illustrate one way that a vortex track may be lost, i.e., the vortices move out of the sensitive volume of the radar. Other modes are also possible. These are (1) catastrophic decay in which the scattered signal suddenly disappears in all receivers simultaneously, and (2) gradual decay and loss of strength, leading to progressively smaller maximum scattering angles and sensitive volumes. In the latter case the vortex signals disappear gradually and at different times in each of the receivers.

General Remarks

As stated above, one of the goals of the NAFEC test program was to determine how far vortices may travel before they are dissipated. It was hoped that statistical data on vortex lifetime as a function of wind, time of day and aircraft type would be collected at runway 13. In the course of analyzing the data,

however, it became apparent that a large fraction of the vortices were blown out of the sensitive volume before decaying. Consequently, only a selected sample of the data was analyzed in detail. Appendix B contains a summary of all the observed vortex signals.

One persistent difficulty was encountered in long baseline (>500 feet) measurements whenever the receivers were upwind from the transmitter so that the acoustic pulses were propagating into the wind. Under these conditions the wind shear near the ground tended to refract the sound pulses upward so that they did not reach the receiver. The effect was accentuated at runway 13 by the rise in the ground along the runway centerline. When this happened, the direct pulse reference signal was frequently absent, and it became necessary to estimate the reference time by other means (Appendix A). There appear to be at least two ways of dealing with this problem:

1. Elevate the transmitter and the receiver so that the effects of wind shear and ground interference may be reduced.

2. Measure the time delay for propagation with the wind, and correct for the known wind velocity component.

HOT-WIRE ANEMOMETER AND PRESSURE SENSOR TESTS

Anyone who has been near a calm body of water or in a field of tall grass as an aircraft flew over at low altitude has observed a passive ground-based vortex sensor in operation. The highly concentrated, counter-rotating trailing vortices interact with the water surface to form wavelets which propagate along with the vortices as they drift in ground effect. Tall grass exhibits the vortex motion even in moderate wind; initially the wind bends the grass in one direction, then as the vortex moves along, the grass can be bent in the opposite direction, reverting later to its original wind-aligned direction. Observations such as these indicate that passive ground-based sensors should be practical as vortex monitors.

DESCRIPTION OF THE PASSIVE SENSOR EXPERIMENTS

Ground-based hot-wire anemometers and a barocel pressure sensor were tested at NAFEC to determine their suitability as remote vortex sensors. The operation of these sensors is discussed in Appendix D. The hot-wire and pressure sensor data were obtained during 175 flybys: 24 DC-7, 38 B-747, 10 C-5A, 24 B-707/DC-8, 52 C-141 and 27 others (P-3, Lear Jet, DC-3, etc.). Only the results of the DC-7 tests will be discussed here.

The sensors were tripod mounted as shown in Figure 16. The hot-wire sensor was attached vertically to the top of the tripod and aligned to record the air velocity component perpendicular to the aircraft ground track. The barocel sensor (the black box in the figure) was attached to the tripod and its height above the ground was changed after approximately twenty data runs. Location of the sensors relative to the test aircraft is discussed in Appendix E.

A block diagram of the experimental setup is shown in Figure 17. The voltage signals A and B from the anemometers and signal P from the pressure sensor were fed to the processing electronics where the signals were linearized and amplified. Chart recorders were used to record the data which consisted of the analog voltage signals of A, B, P, and the instantaneous algebraic difference of the A and B signals. After the tests were completed the sensors-electronics-recorder combination was calibrated and the recorded voltages transformed to velocity and pressure units. Thus, each data run corresponded to four plots of voltage level versus time, and the data presented in this report resulted from conversion of the voltage plots to pressure and velocity plots. The height of the vortex was determined from the acoustic sensor measurements.

Figure 16. Pan Am 747 over Velocity and Pressure Sensor

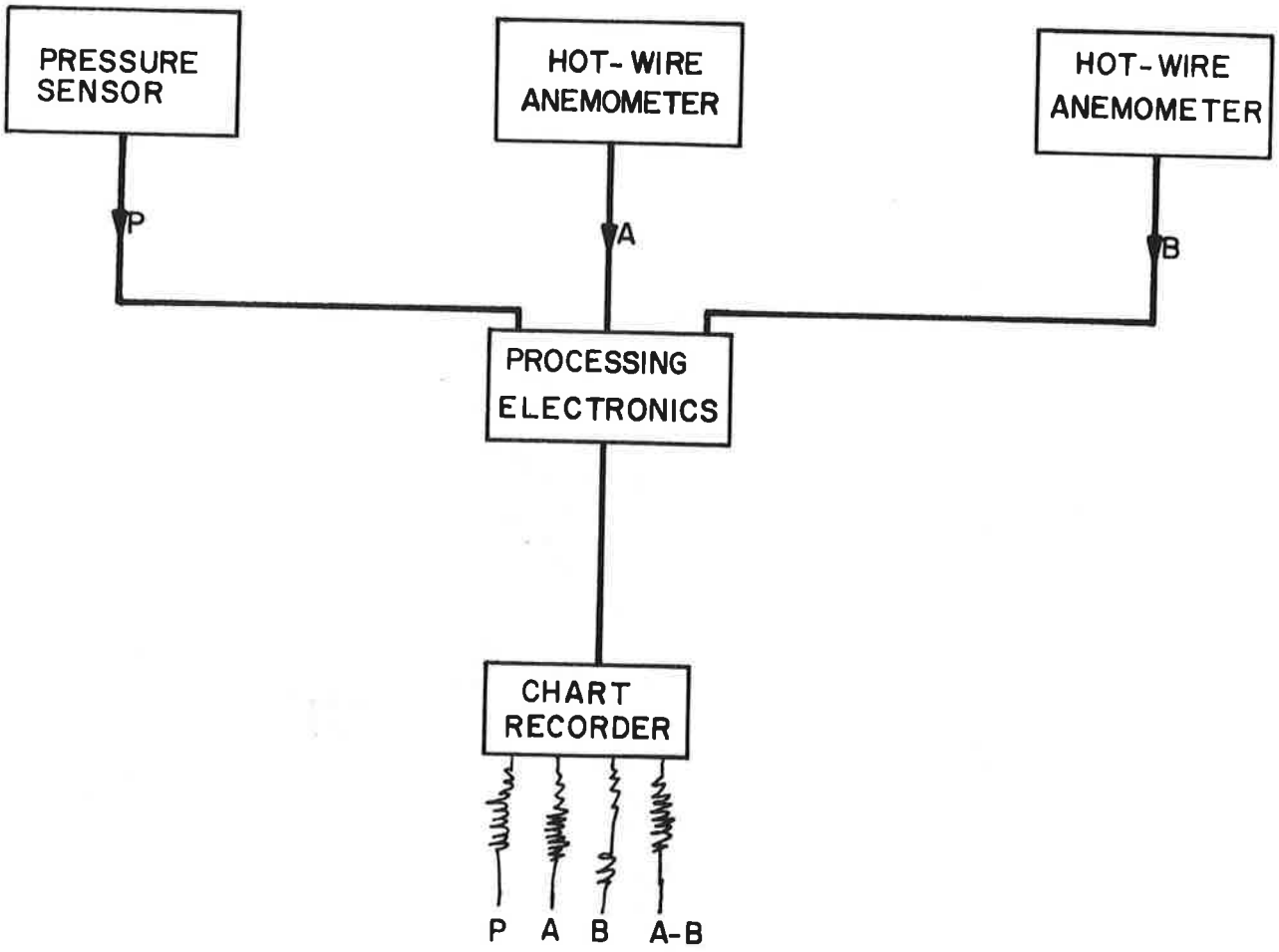

Figure 17. Diagram of Velocity and Pressure Sensor Set-up.

EXPERIMENTAL RESULTS

In order to interpret the data, the measured values were compared to theoretical values obtained from Bernoulli's Principle (See Appendix F). Figures 18 and 19 represent a sample of the data from the DC-7 flights. The "error bars" on the theoretical points indicate the uncertainty in the acoustically measured height of the vortex (typically ±5 feet). Note that for vortices which have descended below 40 feet (12.2 meters) a large disparity exists between the measured and predicted pressure differentials and velocities. The disparity increases as the vortex descends, which suggests that it results from the neglect of viscous decay and vortex breakdown for vortices in ground effect.

The velocity or hot-wire anemometer data exhibits two features: (1) the measured velocity is essentially a constant (about 14 feet/second) and (2) the velocity signature can not be distinguished from ambient winds when moderate turbulence is present or when the wind is changing direction. These features limit the usefulness of hot-wire sensors. Part of the problem could be overcome if three-dimensional velocity sensors were used; in the NAFEC tests only one component of the velocity was measured and it was sensitive to the effects of the changing wind direction. Operationally the hot-wire sensors became contaminated by the dirt thrown up by the aircraft downwash. (At one point, one of the hot-wire sensors was shorted by an insect which was attracted by the radiating heat.)

The pressure sensor, on the other hand, performed well, and the analog signatures of vortices were very easy to distinguish from the ambient noise. The barocel even detected the pressure change caused by the movement of air as the aircraft passed the sensor.

DISCUSSION OF RESULTS

These tests indicate that a matrix of pressure sensors could be used in an airport environment to monitor the existence and horizontal motions of wake vortices near the ground. Such a system would be limited by the ambient wind which determines the maximum height at which a vortex can be detected. When the wind speed is comparable to $\Gamma/\pi h$, the vortex signature is comparable to the pressure differential caused by the ambient turbulence. Figures 20 and 21 are plots of $\Gamma/\pi h$ and are intended as a guide to the expected operating range of a pressure sensor. For instance, when the winds are above 20 feet/second, vortices shed from a DC-7 will not be detected if the vortex is 50 feet or more above the ground. If enough pressure sensors

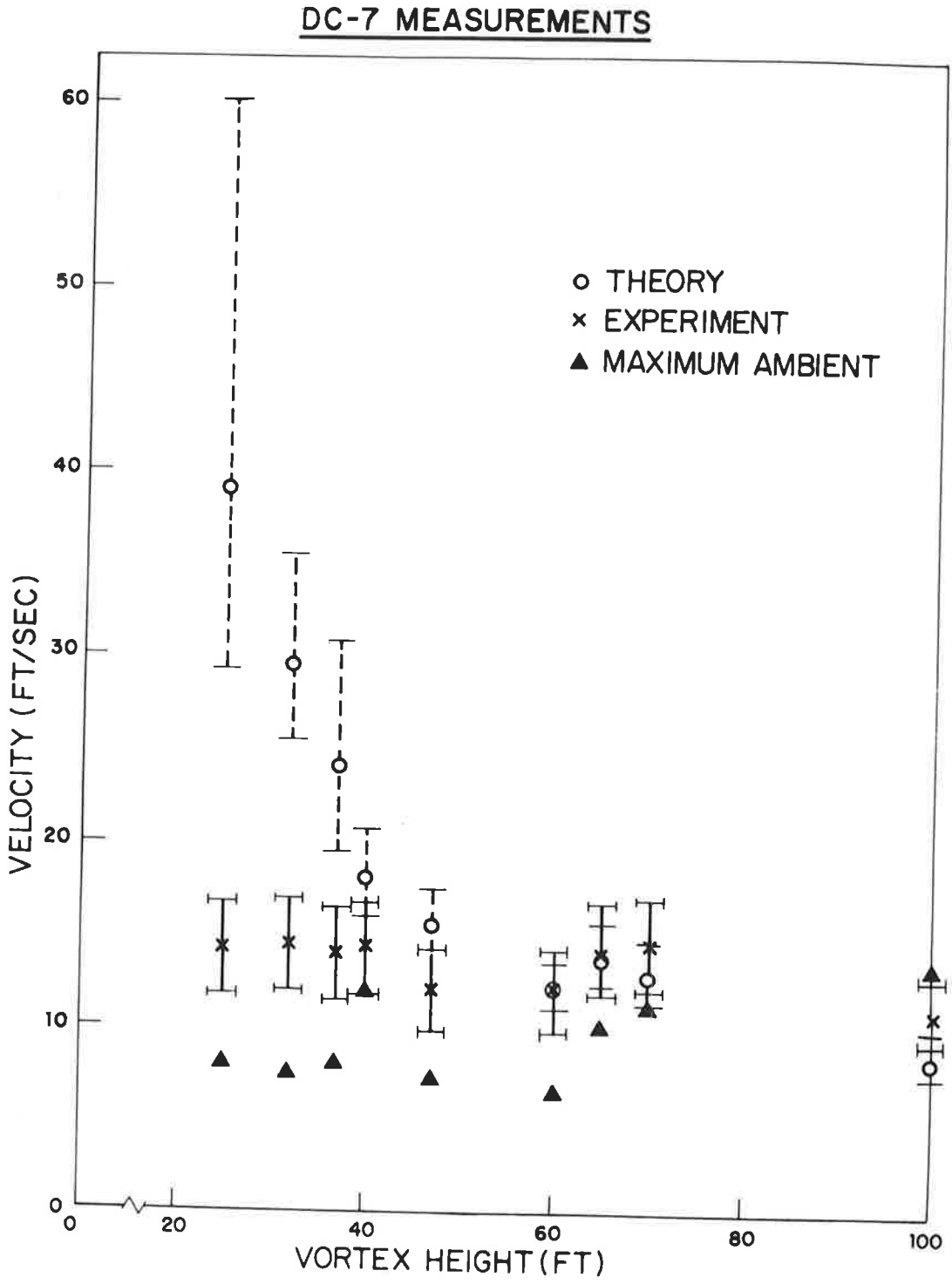

Figure 18. Hot-Wire Anemometer Data

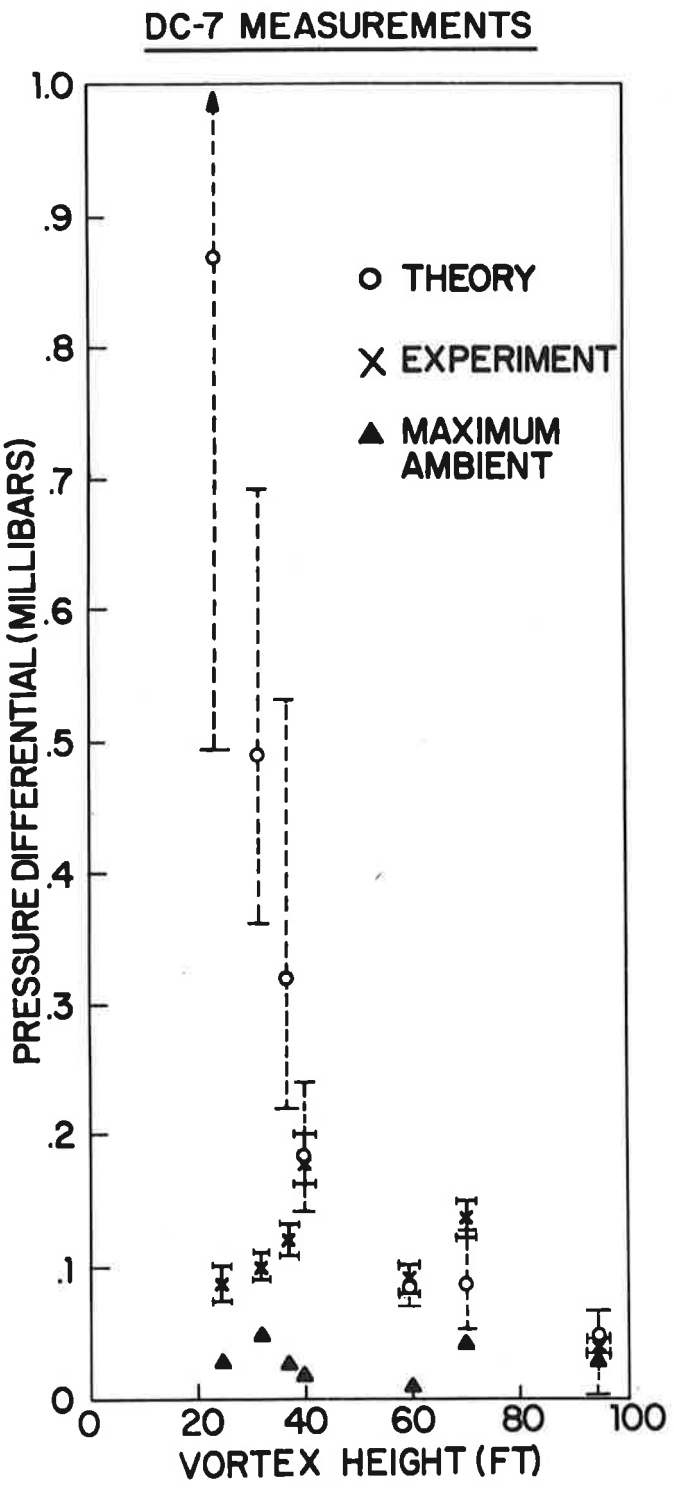

Figure 19. Pressure Sensor Data

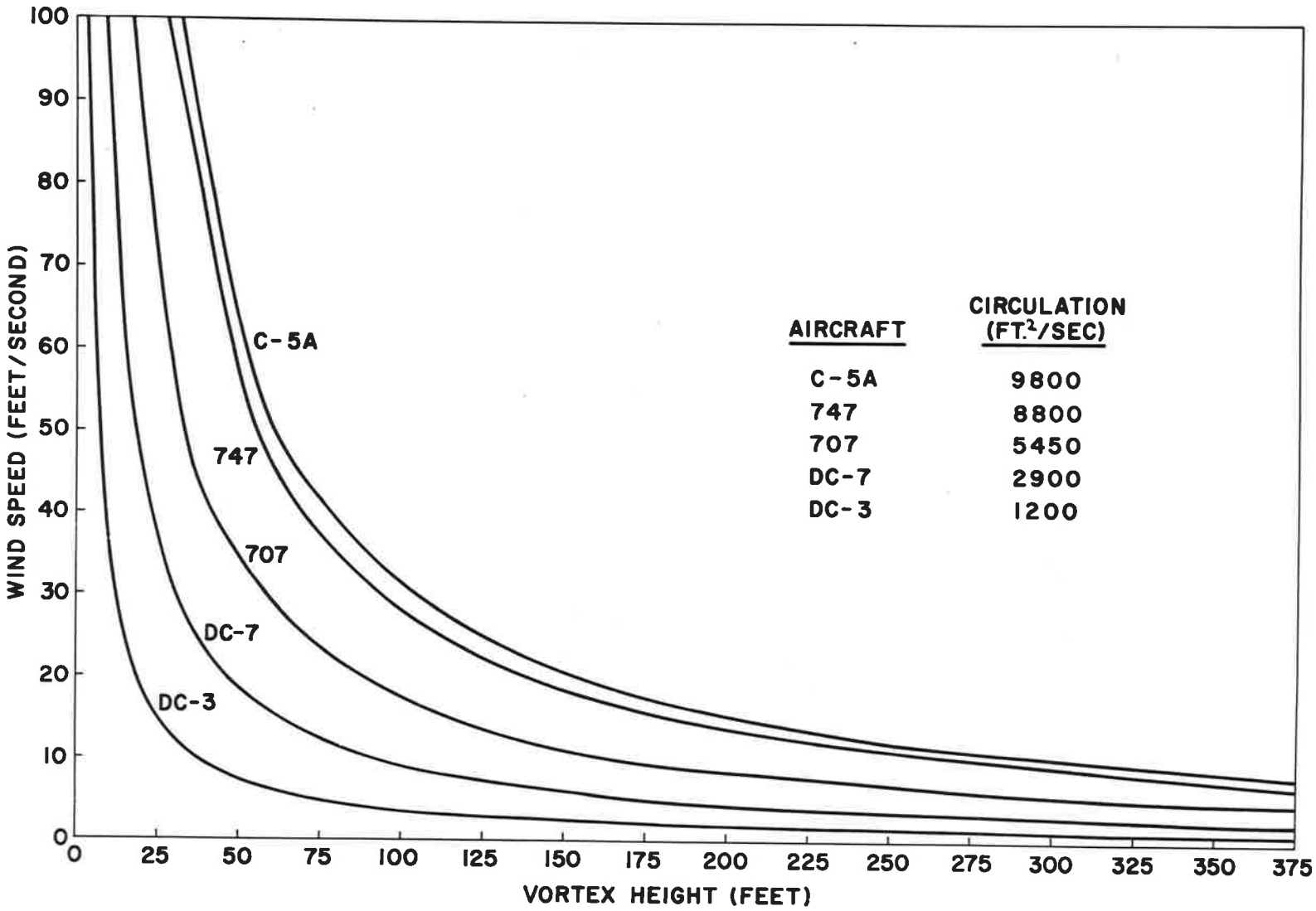

Figure 20. Limiting Ambient Wind Speeds for Pressure Sensor Operation

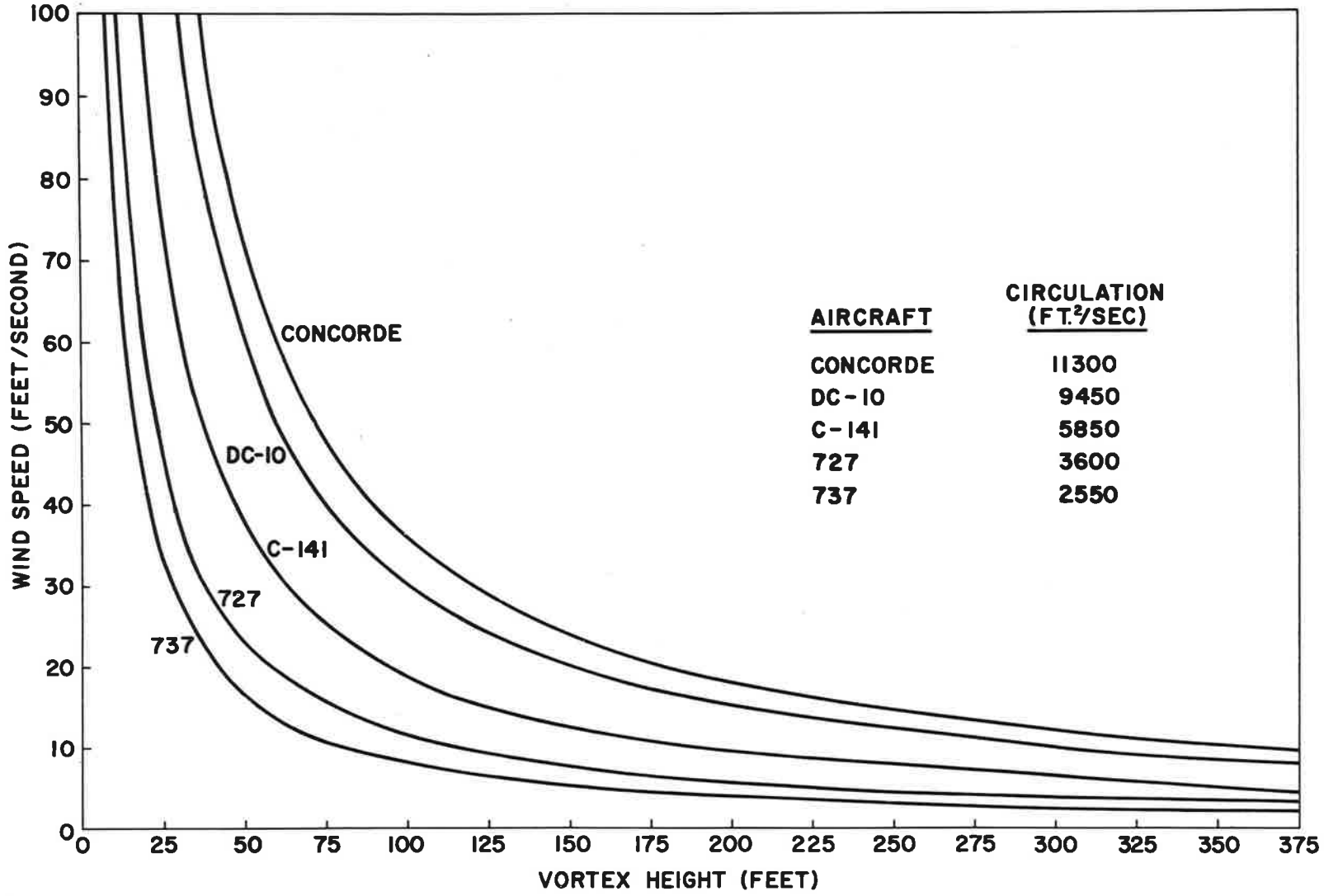

Figure 21. Limiting Ambient Wind Speeds for Pressure Sensor Operation

were used such that a vortex track is detected sequentially by at least four sensors, one conceiveably could calculate the height and effective circulation of that vortex.

It is concluded that pressure sensors may be valuable for monitoring vortices near the ground (at altitudes of the order of a wingspan of the generating aircraft). Possible regions of interest are between parallel runways and near the take-off and touch-down points. When the winds are high, the use of pressure sensors becomes questionable, but the problem should be minimal as the vortices should be swept quickly away and/or dissipated. In other regions pressure sensors complement the acoustic radar, as the acoustic technique performs best when tracking vortices which are at a reasonable height above the ground, where the acoustic path difference is greater.

APPENDIX A

ACOUSTIC DATA ANALYSIS

The procedure for producing vortex tracks, such as those shown in Figure 7, from the recorded acoustic data is outlined in this appendix. The recorded data consist of:

- A timing mark indicating the passage of the aircraft.
- Timing marks indicating when the acoustic pulses were transmitted (pulse spacing ~ 130 ms).
- Acoustic signals from as many as five receivers.

The acoustic signals are composed of the desired pulses (typically 3 ms at 3 KHz) and noise. These signals are filtered by a two-pole, 800 Hz, high-pass filter and recorded. During processing the signals are further filtered by a two-pole, band-pass filter which has a Q low enough to produce minimal pulse distortion ($Q \approx 8$). The resultant signal is then amplified and rectified to produce a dc signal which is applied to the dc-coupled Z-axis (intensity) input of an oscilloscope. The y-axis (vertical) sweep is synchronized to each pulse transmission by means of the pulse transmission timing marks and is swept vertically upward at 20 ms/cm. The x-axis (horizontal) sweep is triggered by the aircraft passage timing mark and is swept from left to right at 5s/cm. The resulting picture (Fig. A-1) shows the time history of the direct signal as a bright streak, roughly horizontal, near the bottom of the frame and the vortex scattered signal as a vertically displaced curved streak. The vertical separation at any value of x is a measure of the scattered pulse delay at the corresponding time. Figure A-1 shows representative records obtained from each of the five receivers for run 27 of 2/14/71 (see also Fig. 7). It should be noted that the data for receiver R_5 is of very poor quality as a result of an open circuit in the tape recorder channel.

In order to transform the data recorded on these "vortex acoustograms" to vortex tracks in the plane of the radar, it is necessary to select a position for the reference arrival time of the direct pulses. Normally, this would be the lower edge of the horizontal band shortly after the aircraft passed. Unexpected difficulties were encountered at NAFEC runway 13, however, due to a hump in the ground along the center line which increased the ground attenuation of the direct pulses to such an extent that they were often lost in the noise at the receiver. Such was the case, for example, with record R_3 of Figure A-1.

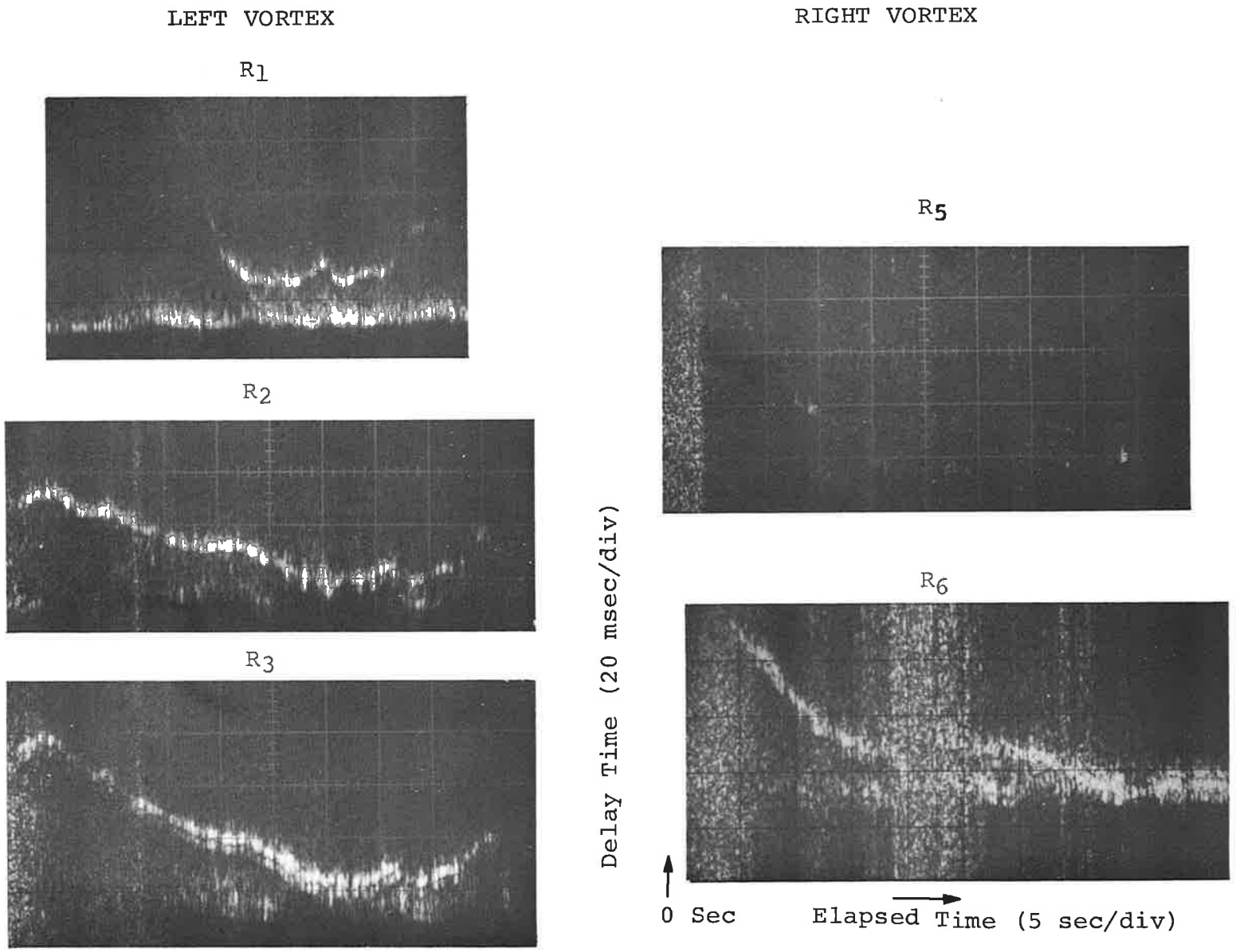

Figure A-1. Acoustograms for Run 27, 7/14/71

Having determined a reference time, by whatever means available, one then measures the delay of the scattered pulse from the acoustogram for selected elapsed times. Representative data are tabulated in Table A-1.

A set of tracking data, consisting of two time delays together with two corresponding transmitter-receiver baseline lengths are entered into a computer program which finds the vortex location by solving for the intersection of two ellipses of constant time delay. Some reduction of random error is achieved by averaging together three positions at adjacent times. The time delay data labeled t_5 and t_6 in Table A-1 were used in this way to produce the right-hand vortex track of Figure 12.

Analysis of the left-hand vortex data (t_1, t_2, t_3) was complicated by the unreliability of the direct pulse transmission for R_3. The procedure adopted was to analyze the more reliable (t_1, t_2) data to obtain the vortex track for elapsed times later than 28s (circles in Fig. 12). The reference time for R_3 was then adjusted to give reasonable agreement between vortex locations determined using (t_2, t_3) and (t_1, t_2) at the same elapsed time. This reference time was then used to find the vortex track from (t_2, t_3) data (crosses in Fig. 12) for elapsed times less than 28s.

TABLE A-1: TIME DELAY DATA, RUN 27, 7/14/71

(Note: t_n is the time delay recorded with the n^{th} receiver)

Elapsed Time (sec)	t_1 (msec)	t_2 (msec)	t_3 (msec)	t_5 (msec)	t_6 (msec)
4				78	60
5				72	56
6				67½	51
7		61	40	65	48
8		64½	42	59	44
10		61	42		32
12		53	35	35	25½
15		49	35	23	17½
18		37	29½		
20		33	25		
23		28½	22		
25		26	22		
28	71	25	21	19	13½
29	56	22			
30	51	20	17		12
31	38	18			
32	26	14½	13		5
33	23	11½			
35	16½	9	9		2
37	15	9½	9½		
40	19	12	11		
41	22	14½	14		

TABLE A-1: TIME DELAY DATA, RUN 27, 7/14/71 (Cont.)

Elapsed Time (sec)	t_1 (msec)	t_2 (msec)	t_3 (msec)	t_5 (msec)	t_6 (msec)
43	15½	9	8		
45	19	11½	11		
47	19	14	13		
50	35	25½	25		
Baseline (msec)	390	660	910	520	790

APPENDIX B
DATA SUMMARY: TESTS AT NAFEC RUNWAY 13

The area used for the tests at runway 13 is shown in Figure 4. Transmitter and receiver locations for each day are shown in Figure B-1. Table B-1 contains the time of day and wind conditions for each set of test runs. Table B-2 to Table B-4 list the type of aircraft and the acoustic signals observed for each run.

TABLE B-1. RUNWAY 13 TEST SUMMARY

Date	Running Times	Wind Conditions
7/7/71	12:05-4:00 PM	6-10 Kts 240°-360°
7/12/71	5:42 PM	?
7/13/71	8:41 AM-3:20 PM	5-15 Kts 150°-190°
7/14/71	7:45-11:36 AM	8-20 Kts 230°-330°
7/15/71	6:31-9:53 AM 10:03-11:41 AM	3-10 Kts 330°-040° 220°-300°

TABLE B-3. SIGNAL SUMMARY (7/12/71, 7/13/71) (Cont.)

Run	R_1	R_2	R_3	R_4	R_5	R_6
18 P-747			6-28			
19 P-747			6-31			
20 Const.	17-28					
21 P-747	X					
22 C5A	17-40					
23 P-747	16-33	13-32	10-25	15-32		
24 C5A		10-25				
25 P-747		7-27				
26 P-747		18-31				
27 C5A						
28 P3						
29 P3						
30 P-747						
31 C-141						
32 C-130						
33 C5A						
34 C-141						
35 P-747						
36 C5A						
37 P3						

TABLE B-3. SIGNAL SUMMARY (7/12/71, 7/13/71) (Cont.)

Run	R_1	R_2	R_3	R_4	R_5	R_6
38 DC-8						1
39 C-130						
40 P-747						8-44
41 C-141						
42 C5A	X	X	X		X	15-44
43 DC-8						X
44 C-130						X
45 C-141						X
46 P-747						13-42
47 C5A	18-30	18-30	19-29		13-38	22-48
48 C5A						21-47
49 Lear						X
50 DC-8						X
51 P-747						13-50+
52 C-130						

TABLE B-4. SIGNAL SUMMARY (7/14/71, 7/15/71)

Run 7/14/71	R_1	R_2	R_3	R_4	R_5	R_6
1 P-707						
2 P-707						X
3 C141						
4 P-707		X				
5 C141						
6 C141						
7 C141		X				
8 C141		X				
9 C141		X				
10 C141		17-30				
11 C-41	X					
12 P-707	X					
13 C141			X			
14 C141						
15 C141			7-25			
16 P-707			X			
17 C141						X
18 P-707						6-15
19 C141						

TABLE B-4. SIGNAL SUMMARY (7/14/71, 7/15/71) (Cont.)

Run	R_1	R_2	R_3	R_4	R_5	R_6
20P-747	25-33	10-36	4-37			4-39
T21P-747						X
22P-707						
23 C141						X
24P-707						
T25P-747						X
26P-707					X	
27P-747	28-51	6-52	6-52		4-15+	4-55
28P-747	18-26	7-26	6-29		29	14-32
T29P-747						
T30P-747			X			
T31P-747			X			
T32P-747			X			
7/15/71						
1 C141		10-60	8-80+		X	
2 C141	X	10-67	6-67		X	
3 707		28-44	7-93		X	
4 C141		X	15-85		X	X
5 747		37-46	8-75		10-47	X
6 C141		X	7-63		X	X
7P-707		X	10-60		10-28	X

TABLE B-4. SIGNAL SUMMARY (7/14/71, 7/15/71) (Cont.)

Run	R_1	R_2	R_3	R_4	R_5	R_6
8 P-747		10-47	5-72			
9 C141					X	
10 C141					X	
11 C141			6-50+			
12 P747		9-143	6-180+		7-72	7-72
13 P-707			11-44			
14 P-747		10-60	6-60			
15 C141			12-44			
16 C141			9-50+			
17 P-747	X	10-55	6-67		8-25	9-24
18 P-747		X	10-52		X	
19 C141			12-44			
20 P-747		X	5-61		X	
21 C141						
22 P-707						
23 P-747		35-50+	9-56	10-56	7-15	
24 C141			X			
25 C141				X		
26 P-707				X		
27 Lear				X		

TABLE B-4. SIGNAL SUMMARY (7/14/71, 7/15/71) (Cont.)

Run	R_1	R_2	R_3	R_4	R_5	R_6
28 P-747		X	6-60	7-82	8-14	
29 C141				10-50+		
30 C141				7-50+		
31 P-747		X	5-62	7-71	6-43+	
32 C141				7-41		
33 C141						
34 P-707				X		
35 P-747		X	10-50	7-51	X	
36 C141						
37 C141				12-50+		
38 P-707				8-50+		
39 C141				X		
40 C141				X		
41 C141				7-50+		
42 C141				18-41		
43 P-707				9-43		
44 C141				15-50+		
45 C141				10-50+		
46 DC-3		X	7-23	6-30	9-19	
47 P-707				10-50+		

TABLE B-4. SIGNAL SUMMARY (7/14/71, 7/15/71) (Cont.)

Run	R_1	R_2	R_3	R_4	R_5	R_6
48 DC-3				8-25		
49 C141				9-20		
50 P-707						
51 C141		12-33	12-33	7-33		
52 C141				10-43		
53 C141				8-31		
54 C141					X	
55 C141					15-33	
56 C141					16-50+	
57 P-707					13-50+	
58 Cessna					X	
59 C141					X	
60 Gulfs.					7-22	
61 P-707					X	
62 P-747					X	

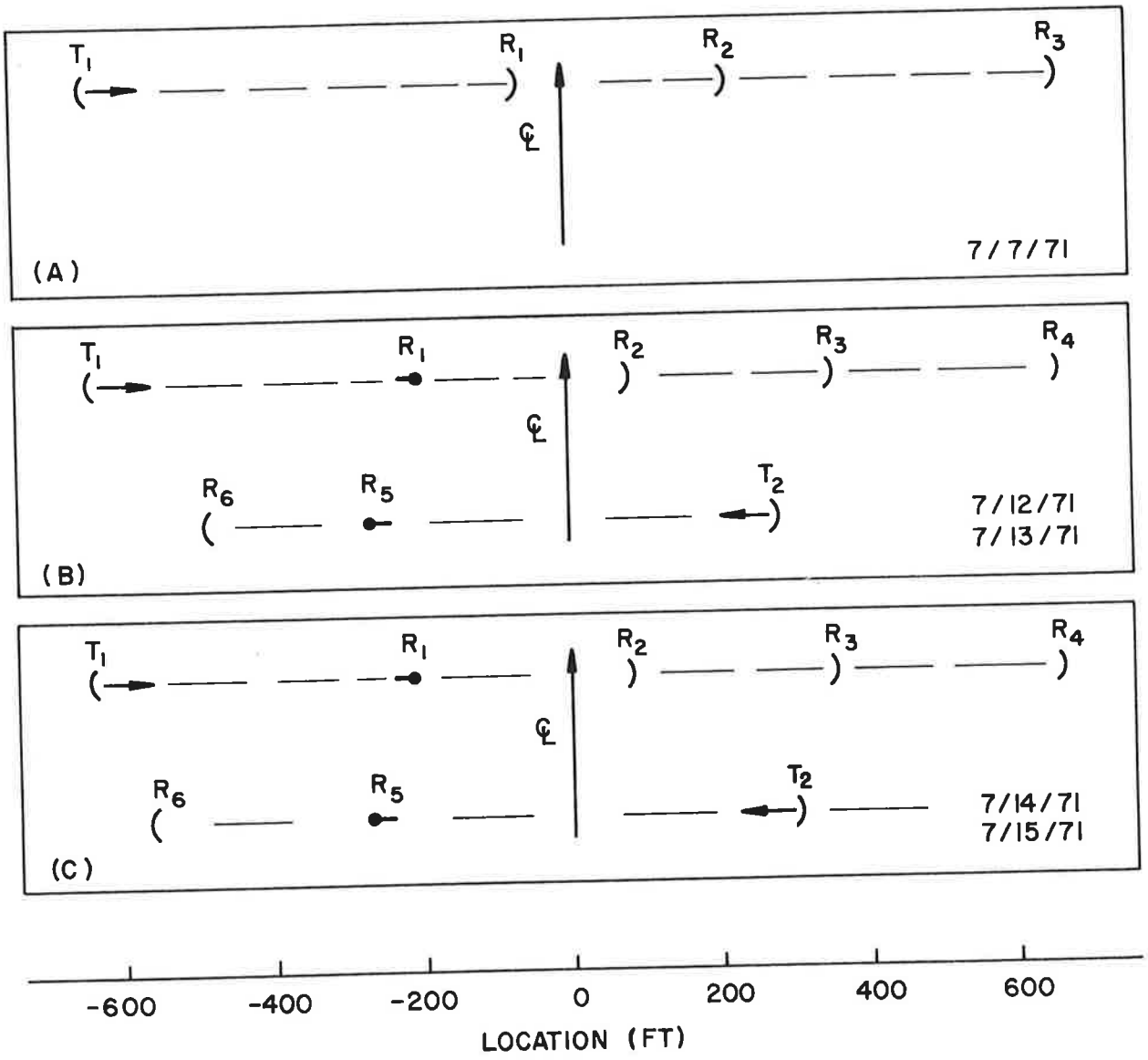

Figure B-1. Transmitter and Receiver Locations for Tests at NAFEC Runway 13.

APPENDIX C
DATA SUMMARY: TESTS AT THE NAFEC TOWER

The tests of the acoustic radar were performed at NAFEC in conjunction with the instrumented tower at a time when the radar was still in an early stage of development. For this reason a number of different experimental arrangements were tried with varying degrees of success. During the course of these tests technical problems arose which have since been resolved, but because they could not be dealt with on the spot, the quality of the radar data is not as good as it could be. The tower tests took place on three separate days during a total of about 3 hrs and 20 mins of aircraft operating time. Details for each day are given in Table C-1.

TABLE C-1. TOWER TEST SUMMARY

Date	Running Times	Wind Conditions
6/15/71	11:25 - 12:05	10-16 Kts 060° - 090°
6/17/71	9:03 - 9:54 AM	1-2 Kts 000° - 070°
7/8/71	9:25 - 11:30 AM	3-12 Kts 290° - 060°

The test layout for 6/15/71 is shown in Figure C-1(a). It consists of a simple two receiver system set up to track the port (upwind) vortex, which was the second one to pass the tower. Table C-2 lists for each run the time intervals over which acoustic signals were recorded, and also contains the tower arrival times and heights as determined from the data for those vortices tracked beyond the tower. Unfortunately, no tower data is available for these runs.

As a supplementary experiment, a microphone in a parabolic dish, which could be scanned in elevation by means of a motor, was located near receiver R_1. It was hoped that the angular position of the vortex could be determined by observing a maximum in either the scattered acoustic signal or in the noise emitted by the vortex. The former proved to be impossible because of the large fluctuations in the scattered signal, but during one run, shown in Figure C-2, the noise generated by a vortex was observed. The vertical noise line appears at a particular value of elevation angle. At 36 sec and 46 sec it had the characteristic swishing sound produced by a vortex.

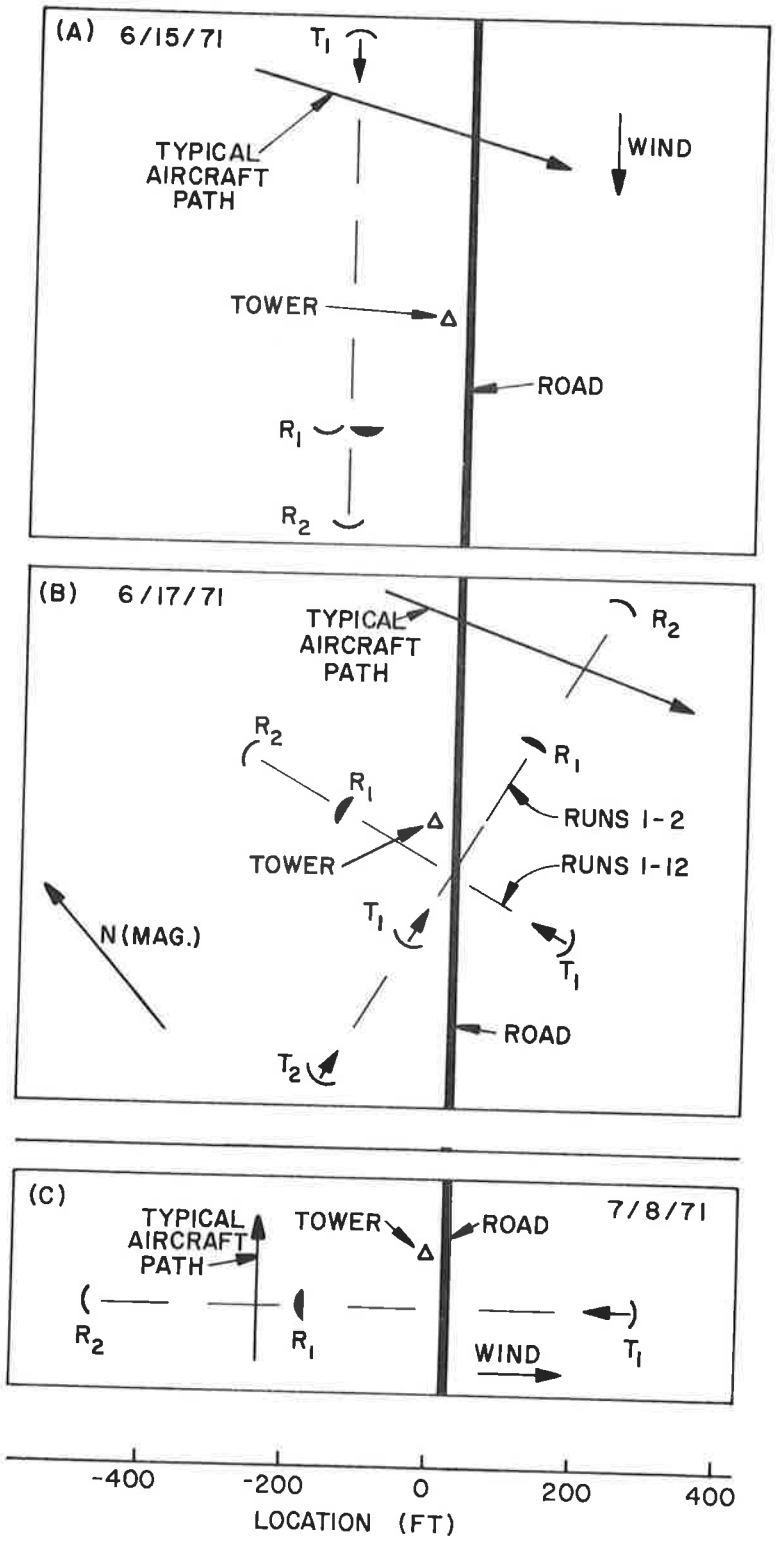

Figure C-1. Experimental Arrangements at the NAFEC Instrumented Tower.

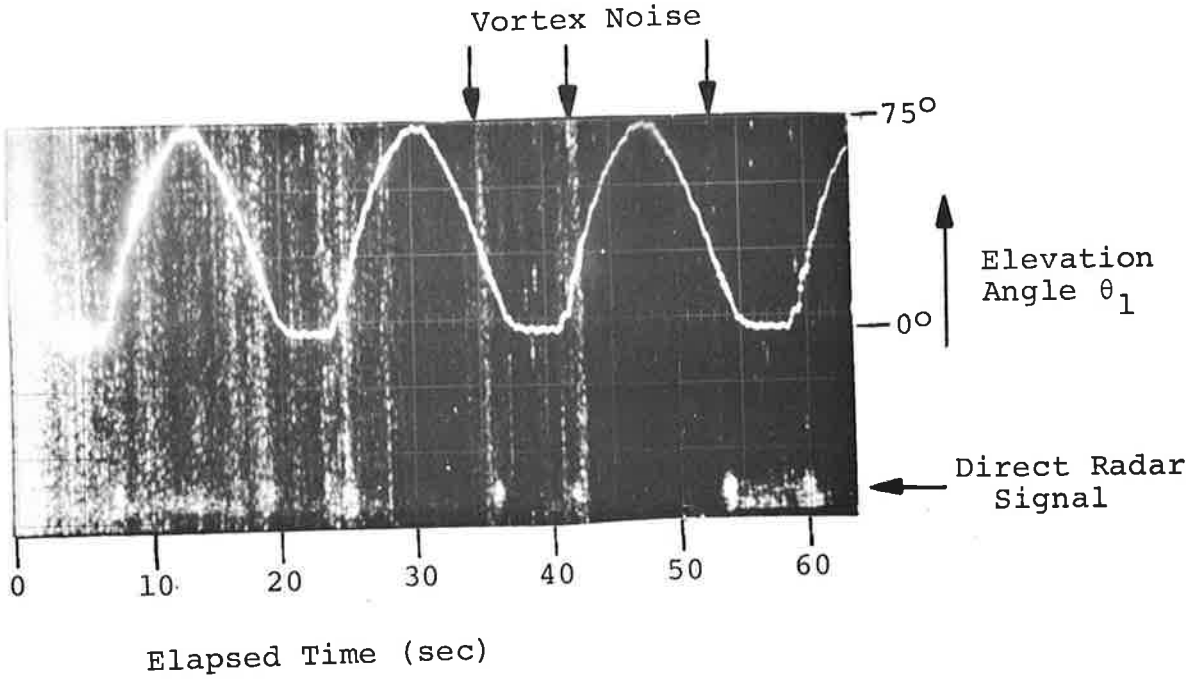

Figure C-2. Acoustic Record from the Passive Scanning Receiver. The Oscillatory Line Shows the Antenna Elevation Angle as a Function of Elapsed Time. Zero Elevation is Determined by the Appearance of the Direct Pulse. Vertical Streaks are Due to Vortex Noise.

TABLE C-2. SIGNAL SUMMARY (6/15/71)

Run	R_1	R_2	Time at Tower	Height at Tower
1	11-44	11-34	20 sec	44 ft
2	4-16	4-12	M	M
3	6-24	7-23	19	77
4	11-19	13-23	20	120
5	10-22	13-17	M	M
6	4-14N	8-11N	A	A
7	13-15, 21-23	X		
8	9-28	9-32	24	66
9	7-22	9-29	A	A

M = missed the tower
A = may not hit the tower
N = noisy

The test set up for 6/17/71 used a more complicated acoustic radar geometry. Two transmitters using different frequencies (3KHz for T_1, 2KHz for T_2) were used with two receivers to observe the starboard (downwind) vortex which was the first to pass the tower. Data were obtained on only two runs (see Table C-3) when a shift in the wind led to a decision by NAFEC personnel to change the direction of the aircraft flight path. The orientation of the acoustic radar system was changed accordingly. Unfortunately, the wind shift proved to be temporary, and the wind quickly reverted to its original direction. Since this baseline shift was already the second one made that morning, it was decided not to move the equipment again but to wait and hope for another wind shift. The remaining runs were thus executed with the aircraft flight path almost parallel to the acoustic baseline. Very little useful acoustic data were obtained that day.

The frustrations of June 17 point out a basic incompatibility between the instrumented tower and the acoustic radar under conditions of light and variable winds. For optimum flow visualization and short vortex arrival times, the tower requires that the aircraft fly in a direction perpendicular to the wind. On the other hand, the acoustic radar baseline must be perpendicular to the flight path so that any major change in direction

means that all the acoustic transducers must be moved, which is no small task.

TABLE C-3. SIGNAL SUMMARY (6/17/71)

	R_1, T_1	R_2, T_1	R_1, T_2	R_2, T_2
1	40-43	12-43	X	18-43
2	X	15-43	X	39-42
3				
4				
5	X	X		
6	26-55	6-57		
7	X	15-45		
8	X	X		
9	X	X		
10	X	X		
11	X	X		
12	X	X		

The third and final series of runs with the tower was conducted 3 weeks later on 7/8/71 with considerably more success. The two-receiver system shown in Figure C-1(c) was set up to observe the starboard (first) vortex. Again the radar had some new experimental features in that the near receiver, R_1, consisted of a parabolic dish with four microphones as shown in Figure C-2(c). (One of the microphones became inoperative and was not used during the tests.) The far receiver, R_2, was conventional, using one microphone in a cylindrical reflector. The purpose of this arrangement was to use the backward response of the microphones to measure the time delay and the response from the dish to determine the elevation angle of the vortex. These angle measurements would then provide an independent determination of the accuracy of the vortex location given by the two baseline system. Unfortunately, the direct ground signal for R_2 was strongly attenuated and could not be measured to give a time reference. The elevation angle data were used instead to determine the correct time reference and therefore

APPENDIX D

DESCRIPTION OF THE PRESSURE AND VELOCITY SENSORS

Pressure measurements were made using a CGS Datametrics Type-1023 Barocel electronic manometer. The pressure sensing element was a high precision, stable, capacitive potentiometer which detects the motion of a thin, highly prestressed metal diaphragm. Positioned between fixed capacitor plates, the diaphragm forms the separation between two gas tight enclosures: one enclosure was connected to an external pressure port; the other was opened to the ambient environment and then sealed before each data run. Used in this manner, the barocel measures the differential pressure. A difference in total pressure within the enclosures produces a force which deflects the diaphragm and the fixed capacitor plates. The sensor is electrically arranged in a 10 KHz carrier excited bridge such that the capacitance variations resulting from deflection of the diaphragm unbalances the bridge and produces a 10KHz voltage whose amplitude is proportional to the pressure differential. (See Figure D-1.)

The velocity measurements, were made using a constant-temperature hot wire anemometer system. A hot-wire anemometer depends upon convection from a heated wire in an air stream; the rate of heat loss from the wire per unit length is proportional to the product of the temperature difference between the heated wire and the air stream and some function of the product of the specific gravity of air and the component of the air velocity perpendicular to the wire axis. The rate at which heat is lost from the sensor is a direct measure of the air velocity.

In the aneomometer circuit, two .001-inch Kovar hot wire sensors are used as two elements of a four element Kelvin bridge. The circuit maintains a fixed current ratio in the two sensors. A feedback amplifier controls the currents, maintaining a fixed voltage ratio across the two sensors, and therefore keeping the resistance ratio fixed even when the ambient temperature changes. As the air flow carries heat from the heated sensor, the bridge becomes unbalanced. The anemometer circuit compensates for the unbalance by feeding current to the heated sensor bringing the resistance ratio close to its original value. This linearized restoring current is the measure of velocity.

The sensors described above were tested near the NAFEC tower during the DC-7 fly byes. The location of the sensors is shown in Figure D-2. In all the tests (DC-7 and others) two

separate hot-wire anemometer systems were placed in tandem along a line normal to the aircraft ground track. The distance between the two hot-wire systems was about "half a wingspan" of the vortex generating aircraft.

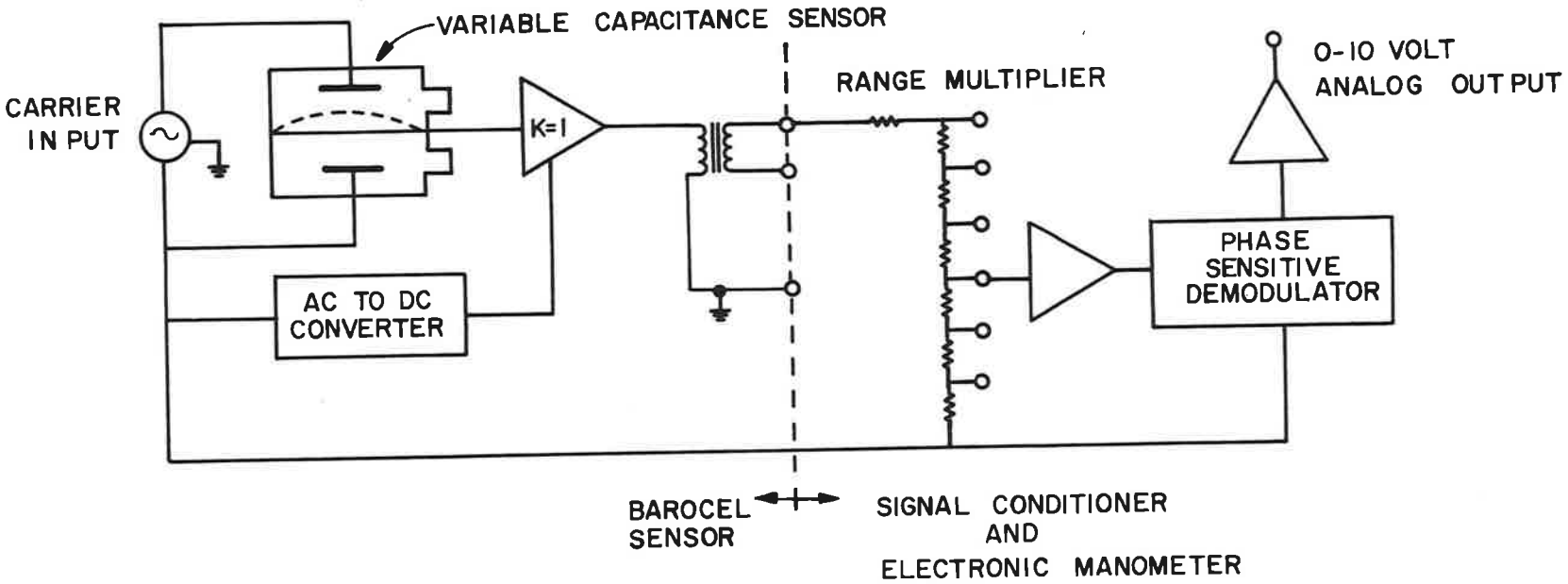

Figure D-1. Variable Capacitance Pressure Transducer

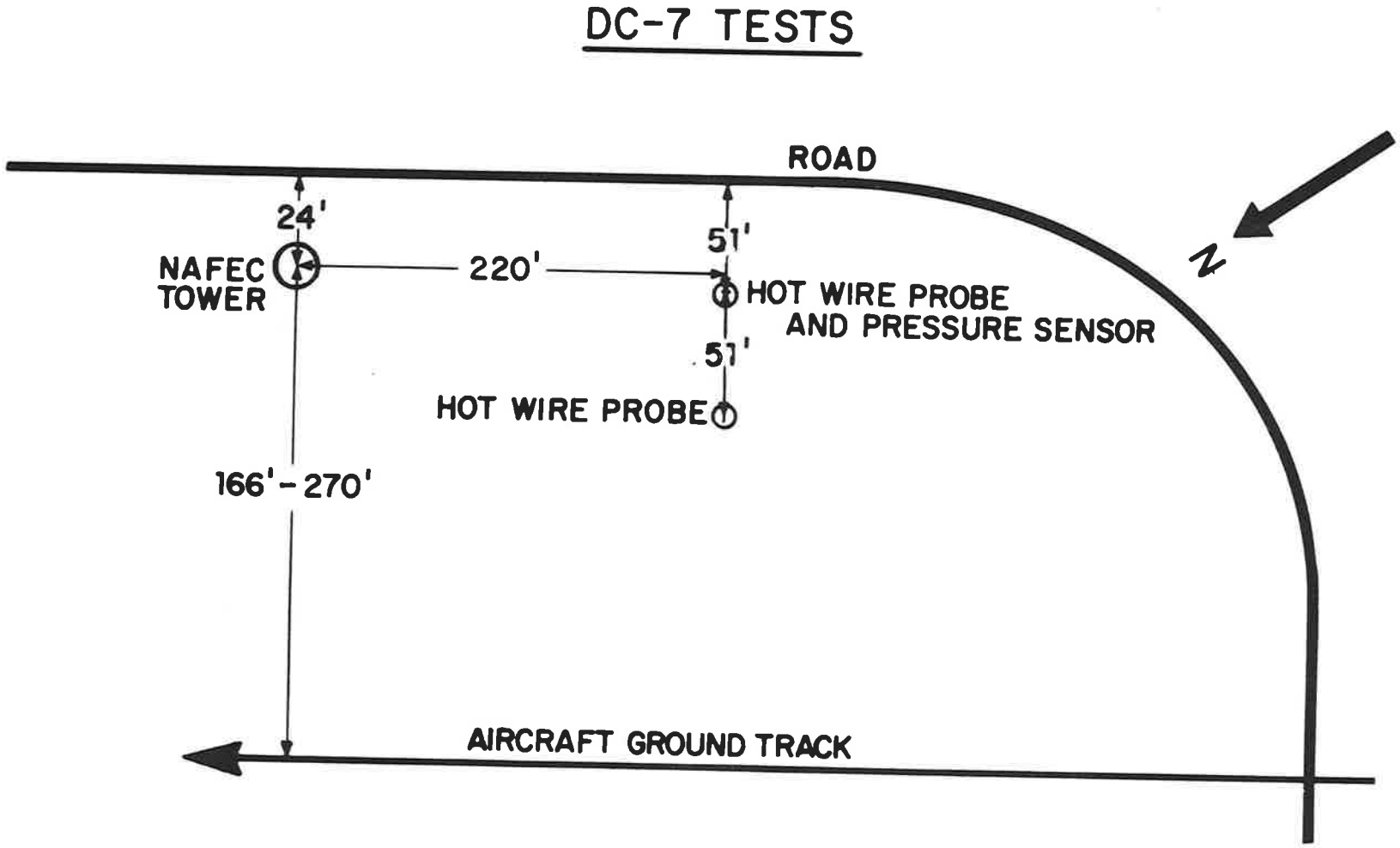

Figure D-2. Sensor Location for the DC-7 Runs

APPENDIX E

VELOCITY AND PRESSURE FIELDS NEAR A VORTEX

DERIVATION OF FORMULAS

By the method of images, a vortex with circulation Γ located a distance h above the ground is equivalent to a system of two counter-rotating vortices in an unbounded region. One of the two is the original vortex; the other is its image, with circulation Γ, a distance h below the ground. The tangential velocity at a distance r from the center of a single vortex is given by

$$V = \Gamma/2\pi r, \qquad r > \text{vortex core size.}$$

To find the velocity at the sensor near the ground when the vortex core is directly above, the velocity contributions from the real vortex and from its image are summed to give

$$V = \frac{\Gamma}{2\pi}\left(\frac{1}{h-d} + \frac{1}{h+d}\right) = \frac{\Gamma h}{2\pi(h^2-d^2)},$$

where d is the height of the sensor above the ground.

In the absence of turbulence, Bernoulli's Principal that the pressure difference is related to the velocity according to

$$\Delta p = \frac{1}{2}\rho V^2,$$

where ρ is the density of the air. With the formula for velocity found above,

$$\Delta p = \frac{1}{2}\rho\frac{\Gamma^2 h^2}{\pi^2(h^2-d^2)^2}.$$

For all theoretical calculations, Γ was determined from the well-known formula for a elliptically loaded wing,

$$\Gamma = (4W)/(\pi b v \rho),$$

where the physical data are:

W = the gross weight of the aircraft;

b = its wingspan; and

v = its speed.

The actual value of Γ is probably less than that calculated using the above formula due to losses occurring during wake roll-up, which in turn is affected by the aircraft configuration.